Contemporary Mathematics
https://ojs.wiserpub.com/index.php/CM/

Research Article

Real-Time Trajectory Modelling of the Mean Tree Volume in a Forest Stand Through a Nonsymmetric Diffusion Process Analogy

Petras Rupšys[1,2,3]

[1]Department of Mathematics and Statistics, Faculty of Informatics, Vytautas Magnus University, Kaunas District, 53361, Lithuania
[2]Bioeconomy Research Institute, Vytautas Magnus University, Kaunas District, 53361, Lithuania
[3]VŠĮ Forest 4.0, Vytautas Magnus University, Kaunas District, 53361, Lithuania
E-mail: petras.rupsys@vdu.lt

Received: 23 July 2025; **Revised:** 5 September 2025; **Accepted:** 25 September 2025

Abstract: This study focuses on the diffusion processes to predict the mean tree volume in a forest stand, considering the variability and uncertainty associated with regional, operational, and environmental factors. The distribution and spatial arrangement of trees within a given forest area, as well as dynamic fluctuations and complex uncertainties, are all represented by the nonsymmetric stochastic differential equations of the Gompertz-type. This study proposes a trivariate system of mixed-effect parameters, Gompertz-type Stochastic Differential Equations (SDEs) that quantify the dynamics of the trivariate distribution of tree size components (diameter, potentially occupied area, and height) against age in a stand. The newly developed model has demonstrated that it is possible to accurately predict, track, and explain the dynamics of mean tree volume yield and growth in a forest stand as trees grow over time. Theoretical findings are demonstrated using observed data from Lithuania's permanent experimental plots that are mixed-species and uneven-aged. The model is implemented using the Maple symbolic algebra system.

***Keywords*:** stochastic differential equation, probability density function, mean tree volume, diameter, height

MSC: 34N05, 60H10, 60H20

1. Introduction

Since volume measurements of standing trees are not realizable in the field, characterizing the tree volume model in a regression expression, which is defined in a different form for any species and region, is common in forestry. Tree volume prediction models are required when there are legal constraints on logging because of the destructive nature of data collection. These models include two predictor variables: diameter at breast height (diameter at the height of 1.3 m above ground) and height, as well as one predictor model with diameter at breast height. Complex modeling paradigms encompass various levels of detail, focusing on accurate long-term forecasting or the interpretation of mechanical processes [1–3]. Forecasts of the mean tree and stand volumes are essential for large-scale forest planning and management. Mean tree and stand volume models are imperative to estimate the carbon flux via formalized models [4, 5]. These models begin with carbon fixation in forest biomass and end with CO_2 being released into the atmosphere through natural decomposition or human-caused processes such as combustion [6, 7]. Regression equations describe

DOI: https://doi.org/10.37256/cm.7120267962

individual-tree and stand-level models as the most widely used type of growth and yield model in management. These equations determine the basal area, volume, mortality, dominant height, and stem density; unfortunately, most of these equations do not reveal continuous changes with stand age.

Because all the models are only as good as the data and techniques that support them are, forest managers must be fully aware of the limits of modeling approaches before concluding the management strategy of a specific stand. Growth and yield models, which are quantitative and often technically complex, are sometimes used to justify the aura of a specific author. The main drawback of regression models is the need for more flexibility due to overfitting, homoscedasticity, multicollinearity, data dynamism, nonnormality, variability, and the assumption of model specification [8–10]. The mechanisms controlling growth can be integrated via process-based models that explain the development of trees and stands [1, 11, 12].

The most fundamental formalization of individual-tree and whole-stand yield and growth models is deterministic, which is not true in reality because of numerous random disturbances. Consequently, a stochastic system would more accurately represent the development of the forest stand [12–15]. The stochastic differential equations approach was not popular in forest growth modeling because it was challenging to estimate the parameters of the transition probability densities for the majority of situations. Numerous disciplines use stochastic differential equations, including finance, physics, medicine, image processing, meteorology, flood and weather forecasting, and forestry [16–19]. In most applications, a mechanical description of a stochastic system is provided by choosing the drift and diffusion functions of stochastic differential equations utilizing simple parametric functions. Additive or multiplicative-type diffusion functions and exponential or sigmoid-type drift functions were developed for a certain class of stochastic differential equations applied to forest growth studies. These functions are dependent on specific fixed- and random-effect parameters. Traditional multivariate models are, unfortunately, limited by the computationally costly process needed for parameter estimation, despite their considerable advantages in capturing time-varying dynamics and covariate effects [20, 21].

The dynamics of forest yield and growth models are integral tools for understanding and forecasting how forests react to changes in the global environment. A theoretical, probabilistic model of forest dynamics is superior to the commonly used deterministic growth models in applied forestry and may reduce uncertainty in long-term predictions of forest dynamics under global change.

Building on previous research, this paper develops a sigmoidal mixed-effects 4-parameter Gompertz-type trivariate stochastic differential equation to produce a growth model and applies it to describe the dynamics of the mean tree volume of both dying and living trees in a forest stand. One of the biggest challenges facing the scientific community in the context of rapid climate change is forest mortality, coupled with the release of CO_2 into the atmosphere. The mean tree volume trajectory for both live and dying trees is newly developed in this work; as a result, the model that was presented enables the tracking and evaluation of carbon dioxide absorption and release in a forest.

The present research initiative focuses on simulating mean tree volume yield and growth dynamic patterns. The static growth models of individual-tree and whole-stand volumes have been extensively studied [22–24]. This work concentrates on the diffusion process analogies provided by stochastic differential equations since commonly used models, such as linear and nonlinear regression models, are unable to adequately capture the intricate relationships between the tree and stand size component variables [17]. The dynamics of the mean tree volume, as well as its increments (mean and current), are investigated in this study concerning the age, height, and potentially occupied area of the trees. The newly developed models were validated using repeated stand measurements in permanent test plots in southwestern Lithuania. The MAPLE framework for symbolic algebra is used to carry out all of the findings [25].

2. Materials and methods

2.1 *Dynamics of tree diameter, height, and potentially occupied area*

The main challenge in modeling tree growth and yield is formulating the trivariate probability density function of the diameter, height, and potentially occupied area of trees in a stand, which varies over age. The trivariate probability density function of tree height, diameter, and potentially occupied area, together with the corresponding regression equation of

individual-tree volume, enables us to define the mean stand volume per hectare, and the two-dimensional probability density function of diameter and height, together with the corresponding regression equation of individual-tree volume, allows us to estimate the mean tree volume in a forest stand. Numerous attempts have been made in forestry to consistently use a probability density function of a bivariate random vector to statistically characterize a stand with a large number of trees [26, 27]. Tree size variables are controlled by the probability density function of the evolutionary type, either univariate or multivariate, which matters for the whole ensemble of trees whose members undergo the same probabilistic growth process [28–30]. In this work, we use a trivariate Gompertz-type stochastic differential equation to describe the evolution of tree diameter at breast height $X_1^i(t)$, tree potentially occupied area $X_2^i(t)$, and tree height $X_3^i(t)$ over age in various M ($i = 1, \ldots, M$) stands in the following Ito's [31] form:

$$dX^i(t) = A\left(X^i(t)\right)dt + D\left(X^i(t)\right)B^{\frac{1}{2}} \cdot dW^i(t), \tag{1}$$

where the exact meaning of the drift term $A(x)$ is as follows:

$$A(x) = \begin{pmatrix} \left(\left(\alpha_1 + \varphi_1^i\right) - \beta_1 \ln\left(x_1 - \gamma_1\right)\right)\left(x_1 - \gamma_1\right) \\ \left(\left(\alpha_2 + \varphi_2^i\right) - \beta_2 \ln\left(x_2 - \gamma_2\right)\right)\left(x_2 - \gamma_2\right) \\ \left(\left(\alpha_3 + \varphi_3^i\right) - \beta_3 \ln\left(x_3 - \gamma_3\right)\right)\left(x_3 - \gamma_3\right) \end{pmatrix}, \tag{2}$$

also the diffusion matrix $D\left(X^i(t)\right)B^{\frac{1}{2}}$ has the following definition:

$$D(x) = \begin{pmatrix} x_1 - \gamma_1 & 0 & 0 \\ 0 & x_2 - \gamma_2 & 0 \\ 0 & 0 & x_3 - \gamma_3 \end{pmatrix}, \tag{3}$$

$$B = \begin{pmatrix} \sigma_{11} & \sigma_{12} & \sigma_{13} \\ \sigma_{12} & \sigma_{22} & \sigma_{23} \\ \sigma_{13} & \sigma_{23} & \sigma_{33} \end{pmatrix}. \tag{4}$$

Here, the independent trivariate Brownian motions are $W^i(t) = \left(W_1^i(t), W_2^i(t), W_3^i(t)\right)^T$, $i = 1, \ldots, M$; given a symmetric matrix B that is positive definite, $B^{\frac{1}{2}}$ is the Cholesky factorization resulting from the transposition of a lower triangular matrix and its counterpart; if $t = t_0$, then an initial status looks like this $X^i(t_0) = x_0 = (x_{10}, \delta, x_{30})^T$ is a degenerate vector $P\left(X^i(t_0) = x_0\right) = 1$; the independent, normally distributed random effects φ_j^i, $j = 1, \ldots, 3$, having zero means and constant variances, respectively $\varphi_j^i \sim N\left(0; \sigma_j^2\right)$, $\varphi^i = \left(\varphi_1^i, \varphi_2^i, \varphi_3^i\right)$; φ_j^i is a random variable that is independent to $W^i(t)$; and the parameters for fixed effects that require estimation are $\theta = (\alpha_1, \alpha_2, \alpha_3, \gamma_1, \gamma_2, \gamma_3, \beta_1, \beta_2, \beta_3, \sigma_{11}, \sigma_{12}, \sigma_{13}, \sigma_{22}, \sigma_{23}, \sigma_{33}, \sigma_1, \sigma_2, \sigma_3, \delta)$. In this setting, α_1, α_2, α_3 are the intrinsic growth rates; β_1, β_2, β_3 are the growth deceleration factors; γ_1, γ_2 , γ_3 is the threshold parameters; σ_{11}, σ_{22}, σ_{33} are the coefficients of volatility; σ_{12}, σ_{13}, σ_{23} are the coefficients of dependency; and σ_1, σ_2, σ_3 are the standard deviations of the normal distribution for the diameter, occupied area and height, respectively.

Stochastic modifications of the Gompertz-type ordinary differential equation are possible in a few distinct ways. This study modeled the randomness of tree diameter, occupied area, and height using a standard Brownian motion. For

the 3-parameter sigmoidal model, the following ordinary differential equation describes a Gompertz-type deterministic trajectory for diameter, occupied area, and height, respectively:

$$dx_j(t) = (\alpha_j - \beta_j \ln(x_j(t) - \gamma_j))\,(x_j(t) - \gamma_j)dt. \tag{5}$$

Thus, assuming that the deterministic parameter, α_j, fluctuates randomly around the mean, $\alpha_j(t) = \alpha_j + \sigma_{jj}W_j(t)$ ($W_j(t)$ is the Brownian motion), the complete deterministic model as defined by Eq. (5) has been transformed into a stochastic model (1).

The forecasts of stand attributes, including mean tree height and mean tree volume, can be significantly impacted by unmeasured environmental factors. Environmental fluctuations, such as changes in temperature, humidity, pollution, and other factors, are fundamental to forest yield and growth. This work incorporates random effects, φ_j^i, $i = 1, \ldots, M$, $j = 1, \ldots, 3$, to account for the impacts of unmeasured forces.

A stochastic differential equations model, in which the relevant parameters are described as random processes of some appropriate form, is a logical extension of a deterministic ordinary differential equations model. This results in a mixed system that contains both stochastic (diffusion part) $\sqrt{\sigma_{jj}}(X_j(t) - \gamma_j) \cdot dW_j(t)$, and deterministic (drift part), $(\alpha_j - \beta_j \ln(X_j(t) - \gamma_j))\,(X_j(t) - \gamma_j)dt$, components, where, in contrast to equation (5), $X_j(t)$ is a stochastic process is a stochastic process instead of a deterministic function. The deterministic component provides sigmoidal growth in tree size variables and describes the growth pattern in which a tree begins slowly, increases in speed to an extremely fast rate, and then slows down once again as it gets closer to maturity. The diffusion component, which produces the diffusion rate, demonstrates that process volatility fluctuates according to the present state of the tree size variable rather than remaining constant.

Applying the transformation $Y^i(t) = \left(e^{\beta_1 t} \ln\left(X_1^i(t) - \gamma_1\right), e^{\beta_2 t} \ln\left(X_2^i(t) - \gamma_2\right), e^{\beta_3 t} \ln\left(X_3^i(t) - \gamma_3\right)\right)^T$ and Ito's formula [31], we can conclude that the trivariate lognormal distribution $LN_3\left(\mu^i(t); \Sigma(t)\right)$ characterizes the solution $(X_1^i(t) - \gamma_1, X_2^i(t) - \gamma_2, X_3^i(t) - \gamma_3)^T$ of our starting stochastic differential equation (1) and that the mean vector $\mu^i(t)$ is defined as follows:

$$\mu^i(t) = \left(\mu_1^i(t), \mu_2^i(t), \mu_3^i(t)\right)^T = \begin{pmatrix} e^{-\beta_1(t-t_0)} \ln(x_{10} - \gamma_1) + \dfrac{1 - e^{-\beta_1(t-t_0)}}{\beta_1}\left(\alpha_1 + \varphi_1^i - \dfrac{\sigma_{11}}{2}\right) \\ e^{-\beta_2(t-t_0)} \ln(\delta - \gamma_2) + \dfrac{1 - e^{-\beta_2(t-t_0)}}{\beta_2}\left(\alpha_2 + \varphi_2^i - \dfrac{\sigma_{22}}{2}\right) \\ e^{-\beta_3(t-t_0)} \ln(x_{30} - \gamma_3) + \dfrac{1 - e^{-\beta_3(t-t_0)}}{\beta_3}\left(\alpha_3 + \varphi_3^i - \dfrac{\sigma_{33}}{2}\right) \end{pmatrix}, \tag{6}$$

the matrix $\Sigma(t)$ of variance and covariance:

$$\Sigma(t) = \left(v_{jk}(t)\right)_{j,\,k=1,\,\ldots,\,3} = \left(\frac{\sigma_{jk}}{\beta_j + \beta_k}\left(1 - e^{-(\beta_j + \beta_k)(t-t_0)}\right)\right)_{j,\,k=1,\,\ldots,\,3}, \tag{7}$$

and the probability density function $f\left(x_1, x_2, x_3, t \,\middle|\, \theta, \varphi^i\right)$:

$$f\left(x_1, x_2, x_3, t \mid \theta, \varphi^i\right) = \frac{1}{(2\pi)^{\frac{3}{2}} |\Sigma(t)|^{\frac{1}{2}} (x_1 - y_1)(x_2 - y_2)(x_3 - \gamma_3)} \exp\left(-\frac{1}{2}\Omega\left(x_1, x_2, x_3, t \mid \theta, \varphi^i\right)\right), \tag{8}$$

$$\Omega\left(x_1, x_2, x_3, t \mid \theta, \varphi^i\right) = \begin{pmatrix} \ln(x_1 - \gamma_1) - \mu_1^i(t) \\ \ln(x_2 - \gamma_2) - \mu_2^i(t) \\ \ln(x_3 - \gamma_3) - \mu_3^i(t) \end{pmatrix}^T (\Sigma(t))^{-1} \begin{pmatrix} \ln(x_1 - \gamma_1) - \mu_1^i(t) \\ \ln(x_2 - \gamma_2) - \mu_2^i(t) \\ \ln(x_3 - \gamma_3) - \mu_3^i(t) \end{pmatrix} \tag{9}$$

All tree size variables (diameter, occupied area, and height) have lognormal-type univariate marginal distributions; moreover, all distributions in two dimensions are also lognormal. The conditional univariate or bivariate distributions of all tree size variables are also lognormal.

2.2 *Dynamics of the mean tree volume*

As a result of the above discussion, the mean tree volume in a stand for various scenarios of tree species ($k \in SP = \{p, s, b\} = \{\text{pine, spruce, birch}\}$), $V_T^k(t)$, may be defined by utilizing the joint probability density function of tree diameter and height:

$$V_T^k(t) = \int_0^{+\infty} \int_0^{+\infty} v_k\left(\frac{x_1}{100}, x_3\right) f_{13}^k\left(x_1, x_3, t \mid \widehat{\theta_{13}^k}, \left(\widehat{\varphi_{1k}^i}, \widehat{\varphi_{3k}^i}\right)\right) dx_1 dx_3, \quad i = 1, \ldots, M, \tag{10}$$

$$f_{13}^k\left(x_1, x_3, t \mid \theta_{13}^k, \left(\varphi_{1k}^i, \varphi_{3k}^i\right)\right) = \frac{1}{2\pi |\Sigma_{13}(t)|^{\frac{1}{2}} (x_1 - \gamma_1)(x_3 - \gamma_3)} \exp\left(-\frac{1}{2}\Omega_{13}^k\left(x_1, x_3, t \mid \theta_{13}^k, \left(\varphi_{1k}^i, \varphi_{3k}^i\right)\right)\right), \tag{11}$$

$$\Omega_{13}^k\left(x_1, x_3, t \mid \theta_{13}^k, \left(\varphi_{1k}^i, \varphi_{3k}^i\right)\right) = \begin{pmatrix} \ln(x_1 - \gamma_1) - \mu_1^i(t) \\ \ln(x_3 - \gamma_3) - \mu_3^i(t) \end{pmatrix}^T (\Sigma_{13}(t))^{-1} \begin{pmatrix} \ln(x_1 - \gamma_1) - \mu_1^i(t) \\ \ln(x_3 - \gamma_3) - \mu_3^i(t) \end{pmatrix}, \tag{12}$$

$$\Sigma_{13}(t) = \begin{pmatrix} v_{11}(t) & v_{13}(t) \\ v_{13}(t) & v_{33}(t) \end{pmatrix}. \tag{13}$$

In Equation (10), $v_k(u, v)$ is the stem volume regression equation, which is based on a q-exponential function [32], $\widehat{\theta_{13}^k}$, $k \in SP$, is the vector of the fixed-effect parameters estimates $\left(\widehat{\alpha_1}, \widehat{\alpha_3}, \widehat{\gamma_1}, \widehat{\gamma_3}, \widehat{\beta_1}, \widehat{\beta_3}, \widehat{\sigma_{11}}, \widehat{\sigma_{13}}, \widehat{\sigma_{33}}, \widehat{\sigma_1}, \widehat{\sigma_3}\right)$ calculated using an approximate maximum likelihood procedure [29], and using method in [29] calibrated random effects $\left(\widehat{\varphi_{1k}^i}, \widehat{\varphi_{3k}^i}\right)$ were computed.

The q-exponential function of tree stem volume is defined as:

$$v_k(u, v) = \tau_1 v^{\tau_2} \left[-\left(1 - \exp\left((1 - \tau_3)u\right)\right)\right]_+^{\frac{1}{1-\tau_3}}, \quad k \in SP \tag{14}$$

here $[a]_+ = \begin{cases} a, & \text{if } a \geq 0, \\ 0, & \text{if } a < 0, \end{cases}$ (τ_1, τ_2, τ_3) is the vector of evaluated parameters, and both u and v are measured in meters.

Table 1 displays the least squares parameter estimates based on a sample size of a few hundred or a few thousand trees that have been felled for different tree species. All the parameters are significant ($p < 0.05$).

Table 1. Parameter estimators (standard errors) of the individual-tree volume Eq. (14)

Tree species	Number of trees	τ_1	τ_2	τ_3
Pine	1,914	0.3269 (0.0285)	1.0597 (0.0195)	0.3711 (0.0046)
Spruce	911	0.1701 (0.0228)	1.2300 (0.0303)	0.3459 (0.0071)
Birch	333	0.2924 (0.0902)	1.0452 (0.0736)	0.3603 (0.0139)

2.3 *Data collection and processing*

Table 2. Summary statistics for tree size variables in the observed dataset

Tree species	Variable	Number of trees	Min	Max	Mean	St. Dev.
Pine	v (cm^3)	6,774	3.03×10^{-6}	4.002	0.41	0.472
	t (year)	36,689	12.0	211.0	53.8	23.6
	d (cm)	36,689	0.1	60.9	19.2	9.5
	p (m^2)	36,689	0.1	124.2	10.1	8.1
	h (m)	6,774	1.3	38.1	17.8	8.5
Spruce	v (cm^3)	3,485	$2.83 \times 10^{-6\text{-}6}$	4.787	0.206	0.412
	t (year)	18,738	8.0	206.0	62.7	22.3
	d (cm)	18,738	0.2	63.6	12.2	8.0
	p (m^2)	18,738	0.1	160.2	9.4	8.2
	h (m)	3,485	1.3	38.0	12.5	8.0
Birch	v (cm^3)	510	$1.57 \times 10^{-6\text{-}4}$	1.891	0.245	0.301
	t (year)	3,270	11.0	127.0	50.9	19.8
	d (cm)	3270	0.8	50.2	15.4	8.7
	p (m^2)	3,270	0.3	173.8	10.2	8.7
	h (m)	510	1.3	31.9	16.1	7.87
All	v (cm^3)	10,796	$2.83 \times 10^{-6\text{-}6}$	4.787	0.337	0.458
	t (year)	58,829	8.0	211.0	56.5	23.4
	d (cm)	58,829	0.1	63.6	16.8	9.6
	p (m^2)	58,829	0.1	173.8	9.9	8.1
	h (m)	10,796	1.3	38.1	16.0	8.7

Plot data were collected from 48 experimental sample plots of mixed-species pine (*Pinus sylvestris*), spruce (*Picea abies*), and silver birch (Betula pendula Roth and Betula pubescens Ehrh) tree stands, which predominate in Lithuanian forests, throughout the municipality of Kazlų Rūda in Lithuania between 1983 and 2020. The data from Kazlų Rūda forests consisted of a range of afforestation time frames, which was a crucial criterion in the selection of simulation data. The sample plots ranged in size from 0.16 to 0.72 hectares and were remeasured between 2 and 6 times at intervals of 2 to 37 years. In the first measurement cycle, how old the ith tree was (i from all trees to the tenth) was determined through the growth core's growth rings (considering even-aged stands, what is recorded). The diameter values were rounded to the closest value of 1 mm, while the plane coordinates had a position accuracy of 1 dm. The height of nearly every fifth tree was measured, with a measurement precision of about 1 dm. When the tree's potentially available area was calculated, the Voronoi diagram's dynamics were considered [33]. For each tree in a plot, the area of the Voronoi polygon was used to assess the potentially available area. Equation (14) was used to calculate the volume of each tree in a plot. Table 2 provides a summary of the measurements.

3. Results

One of the main challenges in forest modeling is properly forecasting long-term changes in the volume of individual trees or whole stands via basic tree size variables such as diameter, height, age, and potentially available area, which are crucial elements that influence tree growth and yield in a forest. The diffusion process described in section 2.1 and the longitudinal remeasurements of trees of different species, ages, and sizes that have been observed allow us to obtain highly accurate yield and growth dynamic curves for various tree species and to examine their features. It is necessary to address the problem of random effects in stand development since stands individually evolve to natural environmental conditions and random perturbations. Considering that the stochastic differential equation approach is used to evaluate a wide range of compound multidimensional issues in numerous fields of mathematical modeling, including forestry, it is reasonable to argue that it is a type of artificial intelligence.

3.1 *Estimation of parameters*

The estimation of parameters is required if we see the sample dataset in section 2.3 as a realization of a trivariate stochastic process, the solution of which has an exact parametric probability density function described by Eqs. (6)-(9). The approximated maximum likelihood estimation procedure [29] for determining values for the fixed- and random-effects parameters of the newly derived probability density function (8) is used in this section. The parameters are set to maximize the approximated log-likelihood that the process described by the model forms the observed data. This work aims to separately estimate the parameters of the tree diameter, potentially occupied area, and height development processes to ensure fast convergence of the approximated maximum likelihood technique in the case of mixed effects scenario. The estimates of the correlations, ($\widehat{\rho}_{12}$, $\widehat{\rho}_{13}$, $\widehat{\rho}_{23}$), between the tree size variables and the volatility parameters, ($\widehat{\sigma}_{11}$, $\widehat{\sigma}_{22}$, $\widehat{\sigma}_{33}$), of the three separate SDE were used to calculate the estimates of the covariances, ($\widehat{\sigma}_{12}$, $\widehat{\sigma}_{13}$, $\widehat{\sigma}_{23}$), as follows:

$$\hat{\sigma}_{kl} = \sqrt{\hat{\rho}_{kl}\hat{\sigma}_{kk}\hat{\sigma}_{ll}}, \quad k = 1, 2, \quad l = 2, 3; \quad k \neq l. \tag{15}$$

The parameter estimates (standard errors) calculated via the approximated maximum likelihood technique using the data described in section 2.3 for both live and dying trees are displayed in Table 3. The diagonal components of the inverse of the observed Fisher information matrix [34] were used to compute the standard errors of the parameter estimations. All estimates of the parameters are significant ($p < 0.05$). For both live and dying trees, Table 4 displays the estimates of the correlations (standard errors) between tree diameter ($j = 1$), potentially occupied area ($j = 2$), and height ($j = 3$). The standard errors of the correlation coefficient estimates are calculated as $\frac{1-\rho^2}{\sqrt{n-3}}$ [35] (n is the number of observed trees).

The intrinsic growth rates (α_1, α_2, α_3) represent the idealized growth dynamics per time unit, assuming exponential population changes. Table 3 reveals that birch trees have the highest intrinsic rate of change in terms of tree diameter, followed by spruce trees and then pine trees. According to Table 3, birch trees have the highest intrinsic rate of change in relation to tree height, followed by pine trees and spruce trees. The stochastic differential equation's volatility amplitudes ($\sqrt{\sigma_{11}}$, $\sqrt{\sigma_{22}}$, $\sqrt{\sigma_{33}}$) show how strong the random fluctuations are. Table 3 indicates spruce trees have the highest growth process fluctuation in terms of diameter, followed by birch and then pine trees; spruce trees have the highest growth process fluctuation in terms of height, followed by pine and then birch trees; and spruce trees have the highest growth process fluctuation in terms of area occupied, followed by birch and then pine trees. Table 4 shows that for all tree species, the highest correlation of tree size variables is between tree diameter and height, while tree diameter and height are almost equally correlated with the area occupied by the tree.

Table 3. Parameter estimators (standard errors) computed from the SDE (1) for live and dying trees

Tree species	Variable	$\widehat{\alpha_j}$	$\widehat{\beta}_j$	$\widehat{\gamma}_j$	$\widehat{\delta}$	$\widehat{\sigma_{jj}}$	$\widehat{\sigma_j}$
All	Diameter	0.0905	0.0252	-6.3143	-	0.0051	0.0074
	($j=1$)	(0.0006)	(0.0002)	(0.079)	-	(0.0001)	(0.0011)
	Area	0.0578	0.0179	-1.3723	1.7773	0.0097	0.0099
	($j=2$)	(0.0005)	(0.0002)	(0.079)	(0.0236)	(0.0001)	(0.0014)
	Height	0.0655	0.0155	-28.358	-	0.0004	0.0024
	($j=3$)	(0.001)	(0.0003)	(0.5052)	-	(1.3×10^{-5})	(0.0003)
Pine	Diameter	0.0815	0.0198	-20.086	-	0.0008	0.0027
	($j=1$)	(0.0005)	(0.0001)	(0.24)	-	(1.3×10^{-5})	(0.0004)
	Area	0.0633	0.0177	-1.9263	1.1978	0.0074	0.0083
	($j=2$)	(0.0006)	(0.0003)	(0.045)	(0.0291)	(0.0001)	(0.0012)
	Height	0.1279	0.0358	-9.5142	-	0.0009	0.0052
	($j=3$)	(0.0008)	(0.0003)	(0.2671)	-	(2.9×10^{-5})	(0.000)
Spruce	Diameter	0.0967	0.0296	-1.5744	-	0.0098	0.0102
	($j=1$)	(0.0011)	(0.0005)	(0.0583)	-	(0.0002)	(0.0017)
	Area	0.0568	0.018	-0.8857	2.1211	0.0131	0.01
	($j=2$)	(0.001)	(0.0004)	(0.054)	(0.0482)	(0.0003)	(0.0017)
	Height	0.0845	0.0245	-3.3976	-	0.0046	0.0065
	($j=3$)	(0.0022)	(0.0008)	(0.2627)	-	(0.0003)	(0.0012)
Birch	Diameter	0.1422	0.0427	-4.7118	-	0.0071	0.0158
	($j=1$)	(0.0022)	(0.0008)	(0.1953)	-	(0.0003)	(0.0025)
	Area	0.0585	0.0177	-2.0636	2.0184	0.0083	0.0093
	($j=2$)	(0.0026)	(0.0011)	(0.1909)	(0.0083)	(0.0005)	(0.0015)
	Height	0.1632	0.04	-37.454	-	0.0005	0.0051
	($j=3$)	(0.0096)	(0.0022)	(0.125)	-	(4.3×10^{-5})	(0.0009)

Table 3. (cont.)

Tree species	Variable	$\widehat{\alpha_j}$	$\widehat{\beta_j}$	$\widehat{\gamma_j}$	$\widehat{\delta}$	$\widehat{\sigma_{jj}}$	$\widehat{\sigma_j}$
				Dying trees			
All	Diameter	0.1813	0.0659	-1.2632	-	0.0192	0.0201
	($j = 1$)	(0.0015)	(0.0006)	(0.0452)	-	(0.0004)	(0.0029)
	Area	0.0555	0.0179	-0.8279	1.7773	0.0115	0.0112
	($j = 2$)	(0.001)	(0.0005)	(0.0383)	(0.0334)	(0.0002)	(0.0016)
	Height	0.1228	0.0364	-3.1174	-	0.007	0.0113
	($j = 1$)	(0.0025)	(0.0009)	(0.188)	-	(0.0004)	(0.0017)
Pine	Diameter	0.1044	0.0292	-7.3251	-	0.0021	0.0067
	($j = 1$)	(0.0009)	(0.0003)	(0.1474)	-	(4.9×10^{-5})	(0.001)
	Area	0.0618	0.0181	-0.9726	1.1978	0.0095	0.0115
	($j = 2$)	(0.0012)	(0.0006)	(0.0471)	(0.0361)	(0.0002)	(0.0017)
	Height	0.151	0.0395	-24.1669	-	0.0003	0.0046
	($j = 3$)	(0.0025)	(0.0005)	(0.8295)	-	(1.6×10^{-5})	(0.0007)
Spruce	Diameter	0.1415	0.0564	-0.5799	-	0.0185	0.0233
	($j = 1$)	(0.0027)	(0.0013)	(0.0552)	-	(0.0007)	(0.0044)
	Area	0.0539	0.018	-0.6066	2.1211	0.015	0.0102
	($j = 2$)	(0.0021)	(0.0011)	(0.0734)	(0.0804)	(0.0007)	(0.0021)
	Height	0.1019	0.0297	-1.2044	-	0.0095	0.0135
	($j = 3$)	(0.0041)	(0.0016)	(0.1618)	-	(0.0009)	(0.003)
Birch	Diameter	0.4667	0.1865	0.0487	-	0.0504	0.0937
	($j = 1$)	(0.0232)	(0.0096)	(0.018)	-	(0.0018)	(0.0305)
	Area	0.0554	0.0177	-2.8847	2.0184	0.0064	0.0091
	($j = 2$)	(0.0055)	(0.0024)	(0.4101)	(0.2102)	(0.0007)	(0.0016)
	Height	0.3191	0.1108	-2.9596	-	0.0121	0.0454
	($j = 3$)	(0.0211)	(0.0066)	(0.7469)	-	(0.0018)	(0.0096)

Table 4. Estimators of the correlation coefficients (standard errors) between tree size variables ($j = 1, 2, 3$) for live and dying trees

Tree species	Live tree			Dying tree		
	$\widehat{\rho_{12}}$	$\widehat{\rho_{13}}$	$\widehat{\rho_{23}}$	$\widehat{\rho_{12}}$	$\widehat{\rho_{13}}$	$\widehat{\rho_{23}}$
All	0.4511 (0.0033)	0.9224 (0.0013)	0.4732 (0.0075)	0.4622 (0.0061)	0.942 (0.0017)	0.5114 (0.0109)
Pine	0.5179 (0.0038)	0.9198 (0.0019)	0.5099 (0.009)	0.5376 (0.0069)	0.9357 (0.0024)	0.5632 (0.0133)
Spruce	0.3732 (0.0063)	0.9487 (0.0017)	0.4376 (0.0137)	0.4234 (0.0116)	0.9551 (0.0022)	0.531 (0.0176)
Birch	0.336 (0.0155)	0.917 (0.0071)	0.2908 (0.0407)	0.2155 (0.0287)	0.906 (0.0134)	0.2013 (0.0717)

3.2 *Dynamics of mean tree volume*

The dynamics of individual tree size variables are the outcome of interactions between trees' neighbors and the surrounding environment, including physical site characteristics, climate changes, air pollution, insect damage, and other factors. To forecast future wood supply and assortment, as well as those associated with sustainable forest stand management, the mean tree volume dynamics must be formalized. The dynamics of a tree's mean volume in a forest stand can be described by the age-dependent relationship, which is defined by Equation (10). Tables 3 and 4 are used to obtain the fixed effect parameters. Furthermore, the mean tree volume equation for mixed-species stands is written with the relative composition of different tree species considered as follows:

$$V_T^a(t) = k_1 V_T^p(t) + k_2 V_T^s(t) + k_3 V_T^b(t) \tag{16}$$

where k_1 is the proportion of pine trees, k_2 is the proportion of spruce trees, and k_3 is the proportion of birch trees. Since the q-exponential function (14) and the lognormal probability density function (11) are continuously differentiable in $\mathbb{R}_2$, the integral (10) exists and has derivatives of the first and second orders. Unfortunately, the integral (10) cannot be expressed in an explicit form, hence all computations are conducted using numerical methods. The dynamics of the live and dying tree's mean volume, as defined by Equation (10), as well as its current volume increment, $cai_T^k(t)$, and mean volume increment, $mai_T^k(t)$, relative increment, $rai_T^k(t)$, and growth acceleration, $ga_T^k(t)$, across the age are defined by:

$$cai_T^k(t) = \frac{d}{dt} V_T^k(t), \tag{17}$$

$$mai_T^k(t) = \frac{V_T^k(t)}{t}, \tag{18}$$

$$rai_T^k(t) = \frac{d}{dt} \ln\left(V_T^k(t)\right), \tag{19}$$

$$ga_T^k(t) = \frac{d^2}{dt^2} V_T^k(t). \tag{20}$$

4. Discussion

Figures 1 and 2 were created to illustrate the distinct growth characteristics of living and dying trees, and to visually demonstrate the evolution of mixed-species forest stands using the given tree size variables (diameter, potentially occupied area, and height). Numerous recent studies have suggested that mixed-species forests may differ significantly from monocultures in terms of growth and structure [36, 37]. In a scenario with fixed effects, where random effects are set to zero, Figure 1 shows the trajectories of the live tree's mean volume, as defined by Eq. (16), as well as its current volume increment, $cai_T^k(t)$, and mean volume increment, $mai_T^k(t)$, relative increment, $rai_T^k(t)$, and growth acceleration, $ga_T^k(t)$, across the age. A comparison of the mean tree volume trajectories of living and dying trees in Figures 1L1 and 1D1 reveals that the volumes of living trees were almost twice as large as those of falling trees. The newly proposed nonlinear model, as given by Eq. (16), has a continuous-time formulation, a sigmoidal shape, and an asymptotic final volume size under both cases of live and dying trees. The implicit (and, in most cases, irrational) assumption that growth never stops is made by non-asymptotic models [38, 39]. As determined by Equation (16), the inflection point of the mean tree volume curve is located at approximately 33% of the asymptotic volume, as shown in Figures 1L1 and 1L4: $\frac{V_T^a(66)}{V_T^a(+\infty)} = \frac{0.4995}{1.5094} \approx 0.331$. The volume's current annual increment for dying trees peaks earlier (approximately in 55 years), but for surviving trees,

it peaks at approximately 65 years, as shown in Figures 1L2 and 1D2. On the other hand, dying trees demonstrate almost two times lower current annual volume increment than live trees do, as illustrated in Figures 1L2 and 1D2. In addition, Figures 1L2 and 1D2 demonstrate that the volume's current annual increment for living trees approaches the mean annual increment (approximately in 105 years) later than that for dying trees (approximately in 85 years). The relative increase in the volume of living and dying trees remained similar over time, as shown in Figures 1L3 and 1D3. Furthermore, as shown in Figures 1L4 and 1D4, the volume growth acceleration (see [38]) of living trees is considerably faster than that of dying trees, and it peaks for both types of trees at roughly the same age (approximately 30 years).

To evaluate the influence of tree size variables, such as height, diameter, and potentially available area, Figure 2 shows the mean tree volume current increment trajectory as a function of the mean tree size variable. The tree volume's current annual increment of living trees over the mean tree diameter, potentially occupied area, and height peaks far sooner than that of dying trees, as seen when comparing Figures 2L1-3 and 2D1-3. Figure 2 shows that the maximum tree volume's current annual increment of living trees (0.0142 m^3yr^{-1}) is almost twice that of dying trees (0.0081 m^3yr^{-1}). When investigating how the mean tree diameter affects the tree volume's current annual increment, we find that the tree volume's current annual increment of living trees peaks considerably later (20 cm), whereas the volume's current annual increment of dying trees peaks at 13 cm (see Figures 2L1 and 2D1). It should be emphasized that the situation is similar when examining how a mean tree's height and potentially occupied area affect the current annual volume increment. Specifically, living trees peak at 11.5 m^2 in terms of the mean potentially occupied area, while dying trees peak at 8 m^2, living trees peak at 20.5 m, and dying trees peak at 17.5 m in mean height (see Figures 2L2-3 and 2D2-3).

It makes practical sense to examine the degree to which the growth of different tree species varies in this experimental area. Plot data were collected from experimental sample plots of pine (*Pinus sylvestris*), silver birch (Betula pendula Roth and Betula pubescens Ehrh), and spruce (*Picea abies*) tree stands that were either pure or mixed species. The examination of Figure 3 validates the general information discussed in Figures 1 and 2. We highlight the most obvious and significant differences in the development processes of different species of trees. The highest asymptote of the mean tree volume for living pine species trees is approximately 1.8 m^3, followed by spruce trees at approximately 0.6 m^3 and birch trees at approximately 0.5 m^3, as shown in Figures 3P1, 3S1, and 3B1. The mean tree volume of dead trees has asymptotes of 0.8 m^3, 0.4 m^3, and 0.1 m^3 for pine, spruce, and birch trees, respectively, which are much smaller than those of living trees (see Figures 3P1, 3S1, and 3B1). Pine and spruce peak in the current annual increment of live trees at approximately the same age of 65, whereas birch peaks at 35 (see Figures 3P2, 3S2, and 3B2). Furthermore, the current annual increment of all tree species is substantially lower for dying trees than for living trees, as shown in Figures 3P2, 3S2, and 3B2. Based on an investigation of the growth acceleration of all the tree species displayed in Figures 3P3, 3S3, and 3B3, we can deduce that the inflection point of a tree volume growth curve for dying trees occurred much earlier than that of living trees.

Because the study characterizes tree growth in terms of a three-dimensional (tree height, diameter, and occupied area) diffusion process, it makes sense to examine the degree to which tree size components affect tree volume growth rates. Overall, Figure 4 shows that the asymptotes of the tree size component trajectory of all variables (diameter, occupied area, and height) of living trees are significantly greater than those of dying trees. Figure 4 shows that the volume growth rate of live trees is the highest for the pine species and the lowest for the spruce species. The rate of the current annual increment in the volume of dying trees was the highest for trees of the pine species and the lowest for trees of the spruce species (see Figure 4 in red). Figures 4P1-3 show that the current annual increment in the volume of live trees for the pine species peaks at a mean tree diameter of approximately 28 cm, a mean potentially occupied area of approximately 12.5 m^2, and a mean tree height of approximately 24 m. Figures 4S1-3 demonstrate that the tree volume current annual increment for live spruce peaks at lower mean tree size variables than that of pine, namely, at a mean diameter of approximately 14 cm, a mean occupied area of approximately 10.5 m^2, and a mean height of approximately 17 m. The current annual increment in the volume of live trees for birch species, as shown in Figures 4B1-3, peaks on average earlier than that for other species. This peak has a mean height of approximately 15 m, a mean occupied area of approximately 6.5 m^2, and a mean diameter of approximately 12.2 cm. In general, Figure 4 allows us to conclude that, for all tree size variables, the volume current increment of dying trees peaks far earlier than that of living trees.

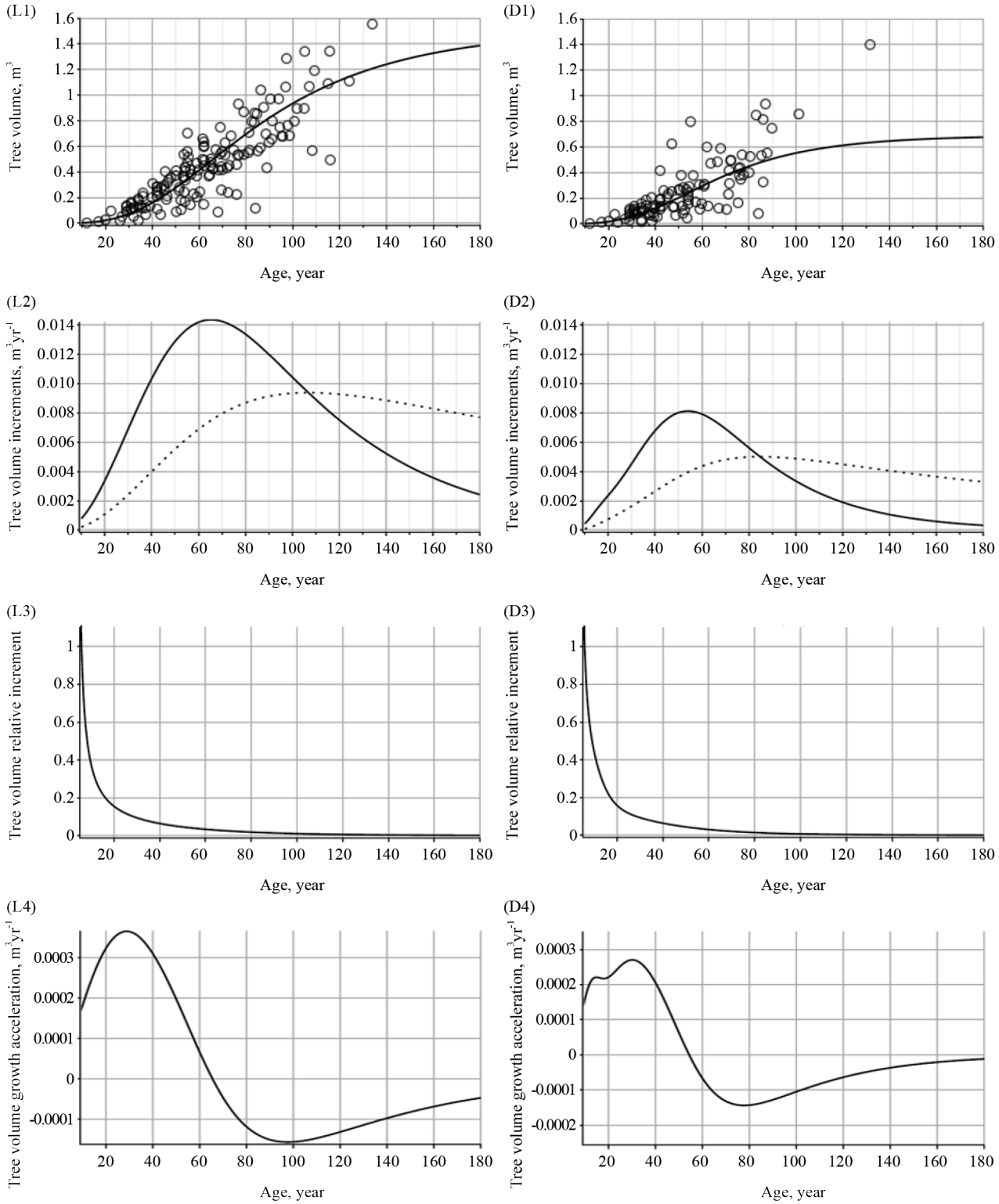

Figure 1. Trajectories of the mean tree volume and its growth for mixed species: (L1, L2, L3, L4) the case of live trees; (D1, D2, D3, D4) the case of dying trees; (L1, D1) the mean tree volume dynamics; (L2, D2) the current (solid line) and mean (dotted line) annual increments of the mean volume of trees; (L3, D3) the relative increments of the mean volume of trees; (L4, D4) the growth accelerations of the mean volume of trees; the mean observed tree volume of the plot is shown by circles

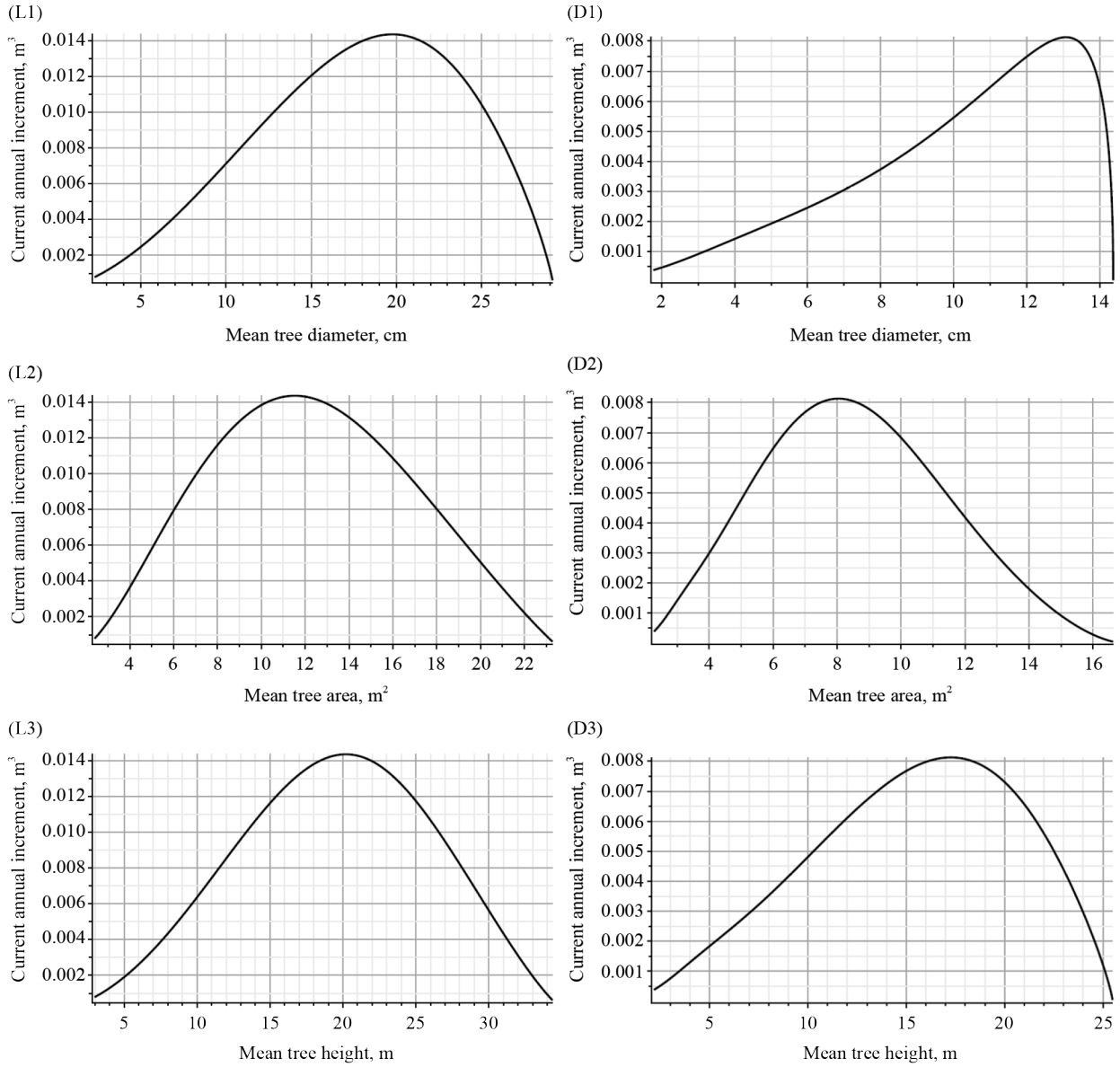

Figure 2. Current annual increments of the mean tree volume for mixed species, live and dying trees: (L1, L2, L3) the case of live trees; (D1, D2, D3) the case of dying trees; (L1, D1) the current annual increment over the mean tree diameter; (L2, D2) the current annual increment over the mean potentially available area; (L3, D3) the current increment over the mean tree height

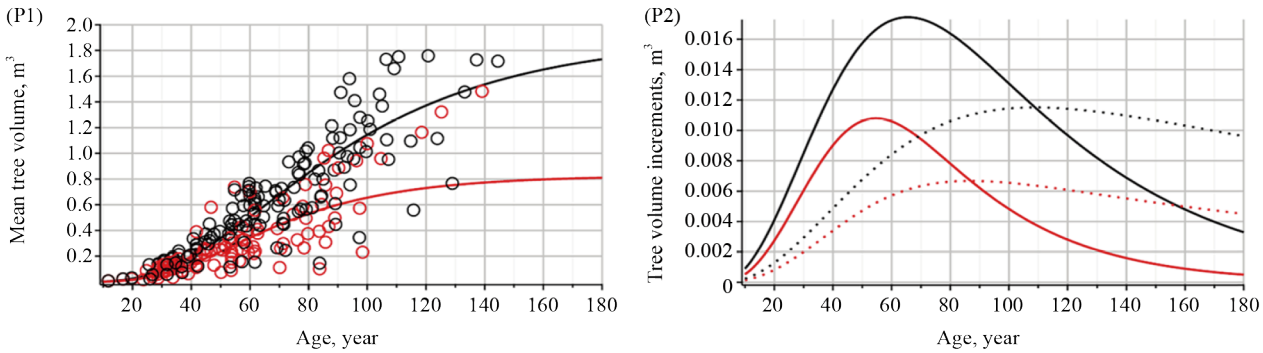

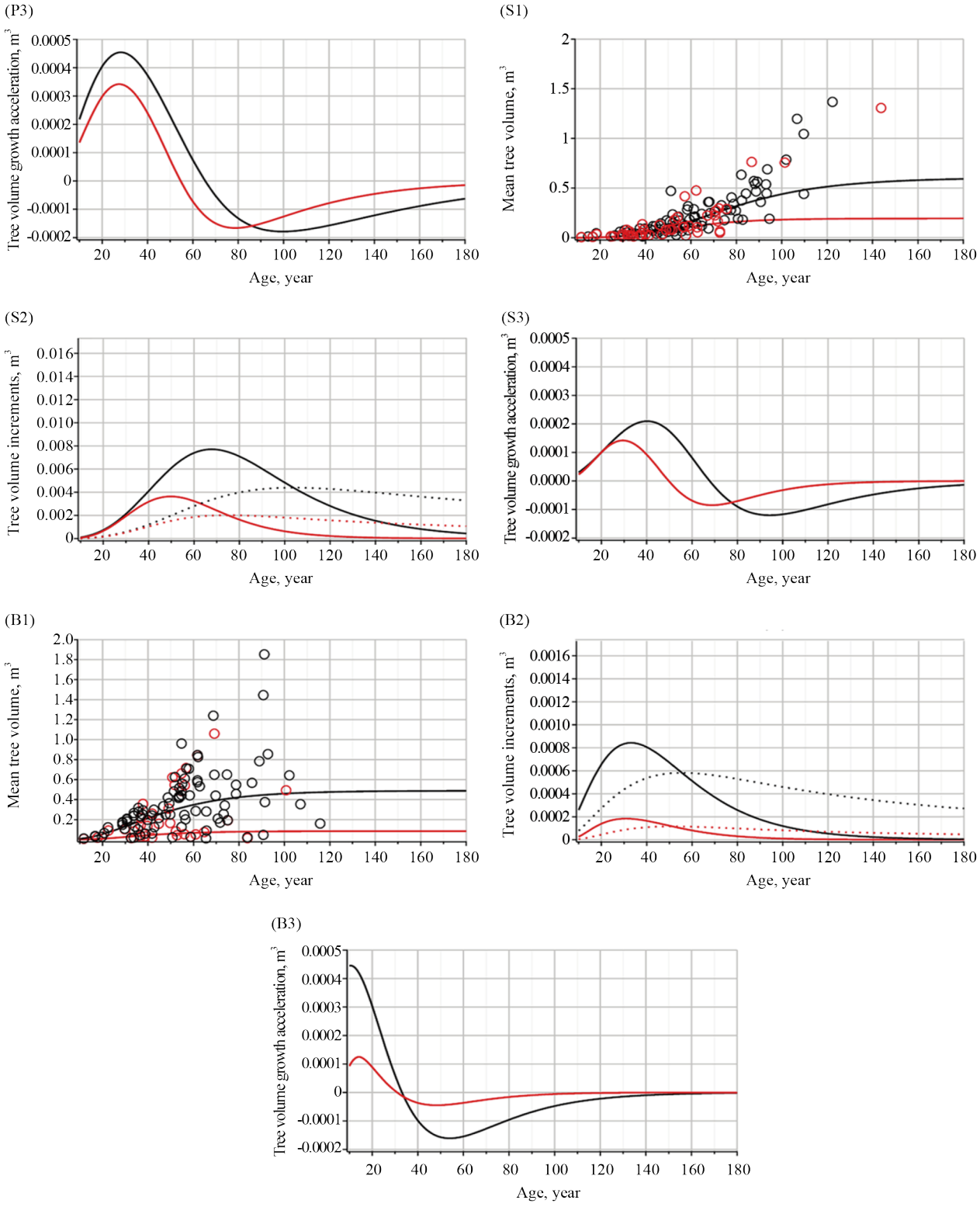

Figure 3. Trajectories of the mean volume of trees, current and mean annual increments, and growth acceleration by tree species of living and dying trees: (P1, S1, B1) the mean tree volume; (P2, S2, B2) the current and mean annual increments of the mean volume; (P3, S3, B3) the growth acceleration of the mean volume; (P1, P2, P3) species of pine trees; (S1, S2, S3) species of spruce trees; (B1, B2, B3) species of birch trees; representation of living trees processes in black; representation of dying trees processes in red; circles demonstrate the plot's observed mean tree volume

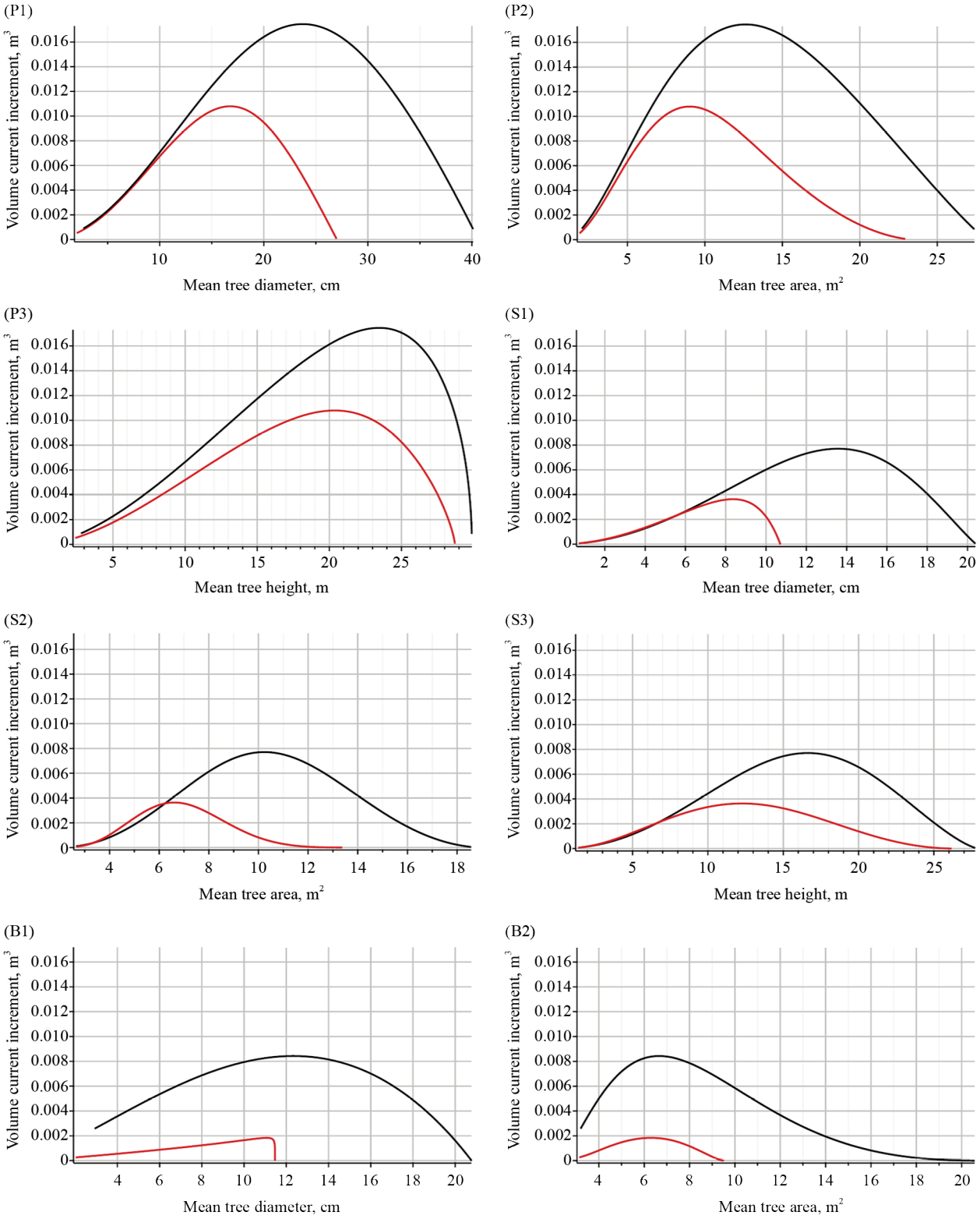
(P1)
Volume current increment, m3
0.016
0.014
0.012
0.010
0.008
0.006
0.004
0.002
0
10
20
30
40
Mean tree diameter, cm
(P2)
Volume current increment, m3
0.016
0.014
0.012
0.010
0.008
0.006
0.004
0.002
0
5
10
15
20
25
Mean tree area, m2
(P3)
Volume current increment, m3
0.016
0.014
0.012
0.010
0.008
0.006
0.004
0.002
0
5
10
15
20
25
Mean tree height, m
(S1)
Volume current increment, m3
0.016
0.014
0.012
0.010
0.008
0.006
0.004
0.002
0
2
4
6
8
10
12
14
16
18
20
Mean tree diameter, cm
(S2)
Volume current increment, m3
0.016
0.014
0.012
0.010
0.008
0.006
0.004
0.002
0
4
6
8
10
12
14
16
18
Mean tree area, m2
(S3)
Volume current increment, m3
0.016
0.014
0.012
0.010
0.008
0.006
0.004
0.002
0
5
10
15
20
25
Mean tree height, m
(B1)
Volume current increment, m3
0.016
0.014
0.012
0.010
0.008
0.006
0.004
0.002
0
4
6
8
10
12
14
16
18
20
Mean tree diameter, cm
(B2)
Volume current increment, m3
0.016
0.014
0.012
0.010
0.008
0.006
0.004
0.002
0
4
6
8
10
12
14
16
18
20
Mean tree area, m2

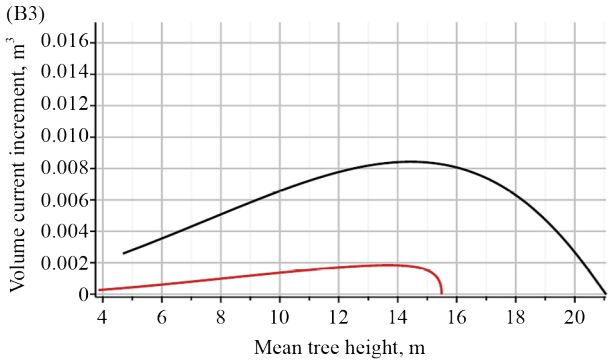

Figure 4. Trajectories of the mean tree volume's current annual increment for all species of live trees and dying trees over tree size variables: (P1, S1, B1) the mean tree volume's current annual increments via the mean diameter; (P2, S2, B2) the mean tree volume's current annual increments via the mean occupied area; (P3, S3, B3) the mean tree volume's current annual increments via the mean height; (P1, P2, P3) species of pine trees; (S1, S2, S3) species of spruce trees; (B1, B2, B3) species of birch trees; representation of living trees processes in black; representation of dying trees processes in red

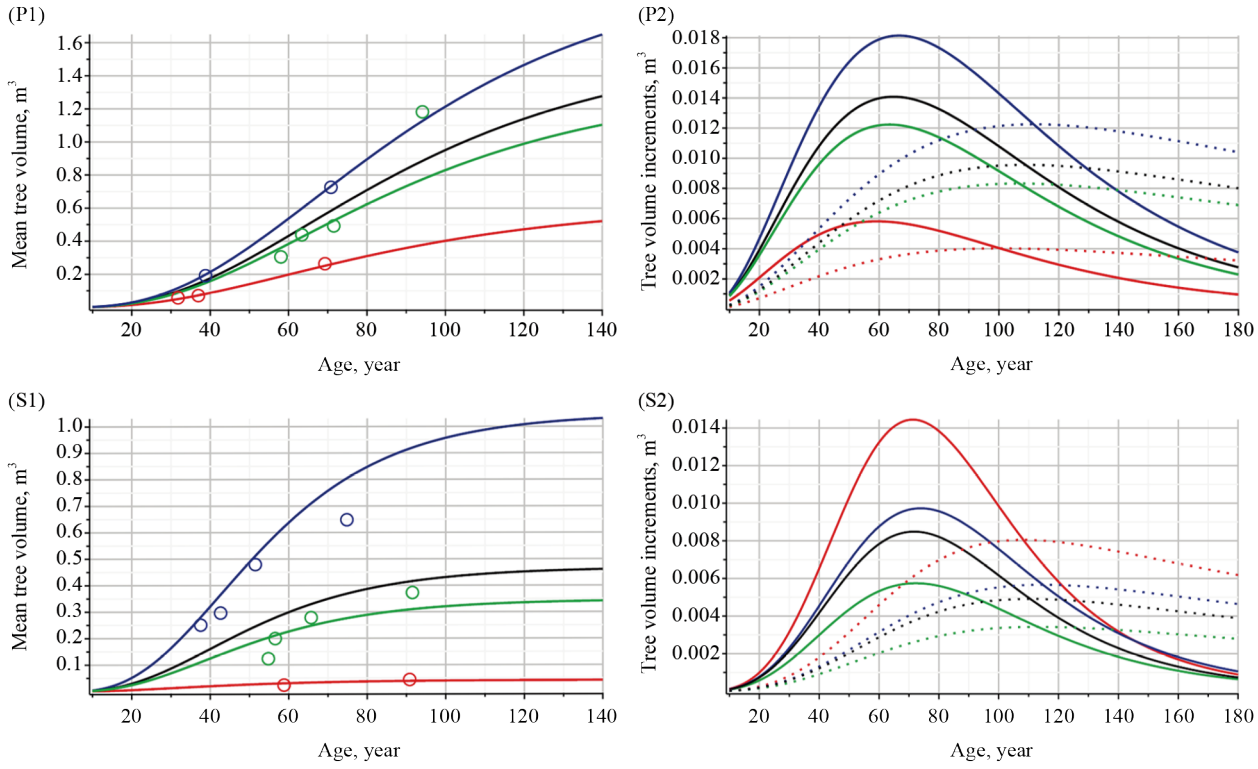

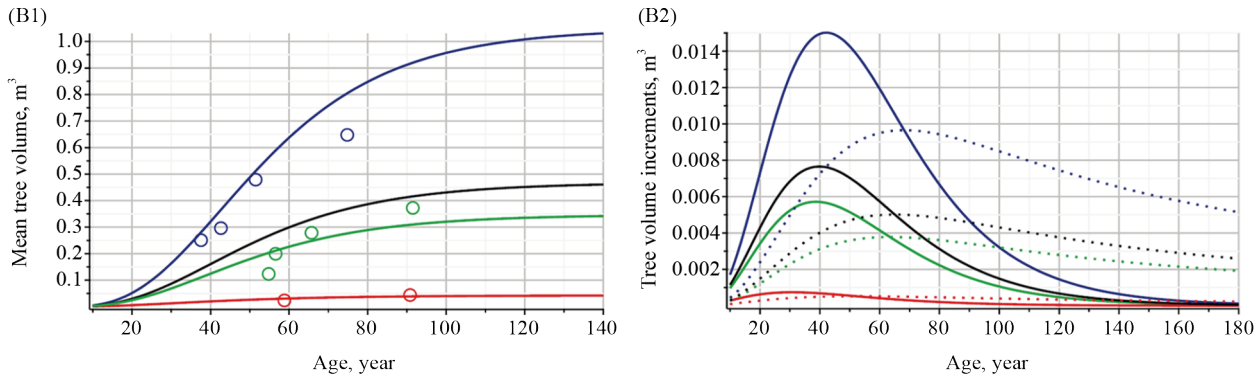

Figure 5. Trajectories of the mean volume of trees and their increments for pine, spruce, and birch species live trees: (P1, S1, B1) the mean volume of trees: in black—fixed effects mode, and in red, blue and green—mixed effects mode for three different plots; in circles—the observed values; (P2, S2, B2) the mean volume's current, and mean annual increments: in black—fixed effects mode, and in red, blue and green—mixed effects mode for three different plots; solid line—current annual increment; dotted line—mean annual increment; (P1, P2) pine species: in red—the first stand (pine 100%); in blue—the second stand (pine 59%, spruce 3%, birch 38%); in green—the third stand (pine 25%, spruce 71%, birch 4%); (S1, S2) spruce species: in red—the first stand (pine 24%, spruce 76%); in blue—the second stand (pine 39%, spruce 51%, birch 10%); in green—the third stand (pine 61%, spruce 3%, birch 36%); (B1, B2) birch species: in red—the first stand (pine 48%; spruce 14%; birch 38%); in blue—the second stand (pine 72%, birch 28%); in green—the third stand (pine 32%, spruce 60%, birch 8%); in circles—observed values

The influence of the plot's random effects on basic tree size variables, such as tree height, tree diameter, and area occupied, will be the main focus in further research, rather than additional environmental variables that characterize climate, soil, and stand topography. From a statistical perspective, the growth processes in each region involve various forms of uncertainty. The random effects arise from the assumption that each forest stand has a random and unobserved impact, where random indicates that the variable is random, and unobserved indicates that we are unable to measure it. Due to the integration of the stand's random effects into the stochastic differential equation (1), environmental random disturbances are inherently incorporated into the tree or stand attribute model. The additional features associated with the tree yield and growth processes in various stands will next be covered. The basis of the fixed effect parameters used to visualize all previous mean tree volume yield and growth models in Figures 1-4 is presented in Table 3. Plot random effects are used in Figure 5 to illustrate the volume and its increments of the mean tree in the plot among the various stands in the region. In Figures 5P1, 5S1, and 5B1, the mean tree volume trajectories are displayed with the observed values for the fixed effect mode (random effects are set to 0) as the black curve and for the three different plots random effects are calibrated (see, Eq. (24) in [29]) as the red, blue, and green curves of the first, second, and third stands, respectively. The asymptotes of the mean tree volume trajectory for pine trees are much greater than those for spruce trees, as shown in Figures 5P1, 5S1, and 5B1. Finally, the asymptotes of the mean tree volume trajectory for birch trees were the lowest. In Figures 5P1, 5S1, and 5B1, the tree volume's observed values in three different plots are circled and show good agreement with the predicted values. Figures 5P2, 5S2, and 5B2 show that trees of the pine species gain the highest current annual increment (as well as the mean annual increment), whereas trees of the birch species achieve the lowest increments. According to the same figures, the age at which the current annual increment peaks varied depending on the stand. For pine species, this age ranges from 57-70 years; for spruce species, it ranges from 55-73 years; and for birch species, it varies from 45-56 years. Furthermore, Figures 5P1, 5S1, and 5B1 highlight that the current annual increment for spruce and pine trees equates to the mean annual increment at approximately 105-115 years of age, whereas for birch trees, this takes place at approximately 70-80 years of age.

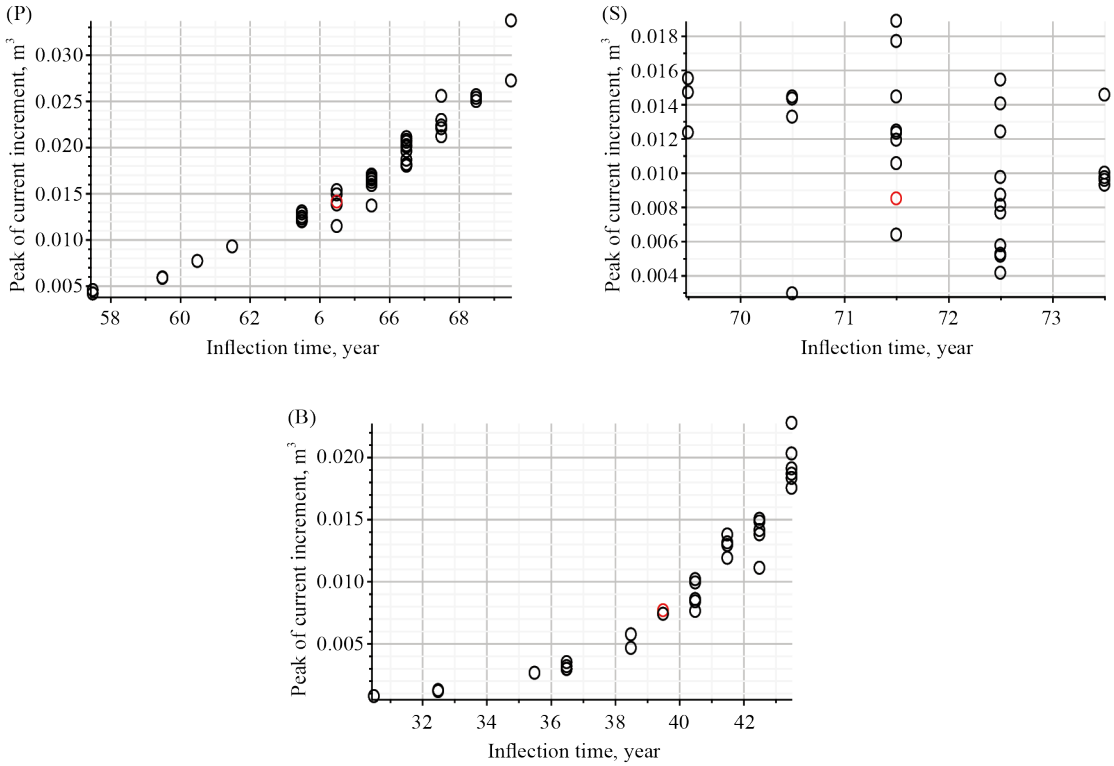

Figure 6. Link of the peak of the volume's current annual increment over inflection time: (P) pine species; (S) spruce species; (B) birch species; red circle indicates the fixed effects scenario

t is essential to take into account that a tree's size characteristics at any given age significantly dictate how much it can grow. Additionally, this study demonstrates that a tree's age can be utilized to model, analyze, and measure its volumetric growth. Suppressed trees are distinguished by lagging a volume current annual increment that lasts longer during growth and has a lower peak, whereas successful trees have a greater current annual increment peak and a later start of growth decline. The link between the growth inflection point and the volume's current annual increment peak is shown in Figure 6. Figures 6P, 6S, and 6B show that for the pine and birch species, as the growth inflection point increased in the plot, the current annual increment in volume increased, whereas for the spruce species, this trend was the opposite. This graphic also shows how the stand species combination, soil quality, tree morphology, and other factors may considerably impact how the trees experience growth in the stand.

Figure 7 shows how the asymptotes of the mean tree diameter, occupied area, and height curves vary substantially for different stands and tree species (looking at the values in Figure 7, where these curves approach the *x*-axis). Figure 7 shows that the current annual increment in the volume of trees reaches a maximum in different plots with different mean tree diameters, occupied areas, and heights. Furthermore, when the mean tree diameter is between 15 and 28 cm, the mean occupied area is between 6 and 19 m^2, and the mean height is between 16 and 23 m, pine trees reach the peak of the volume current annual increment; when the mean tree diameter is between 12 and 20 cm, the mean occupied area is between 8 and 15 m^2, and the mean height is between 15 and 20 m, spruce trees reach the peak of the volume current annual increment; and when the mean tree diameter is between 7 and 22 cm, the mean occupied area is between 7 and 13 m^2, and the mean height is between 9 and 25 m, birch trees reach the peak of the volume current annual increment. The asymptote of the mean tree height and diameter in a plot rises with the highest current annual increment in the volume of the trees in the plot, as shown in Figure 7.

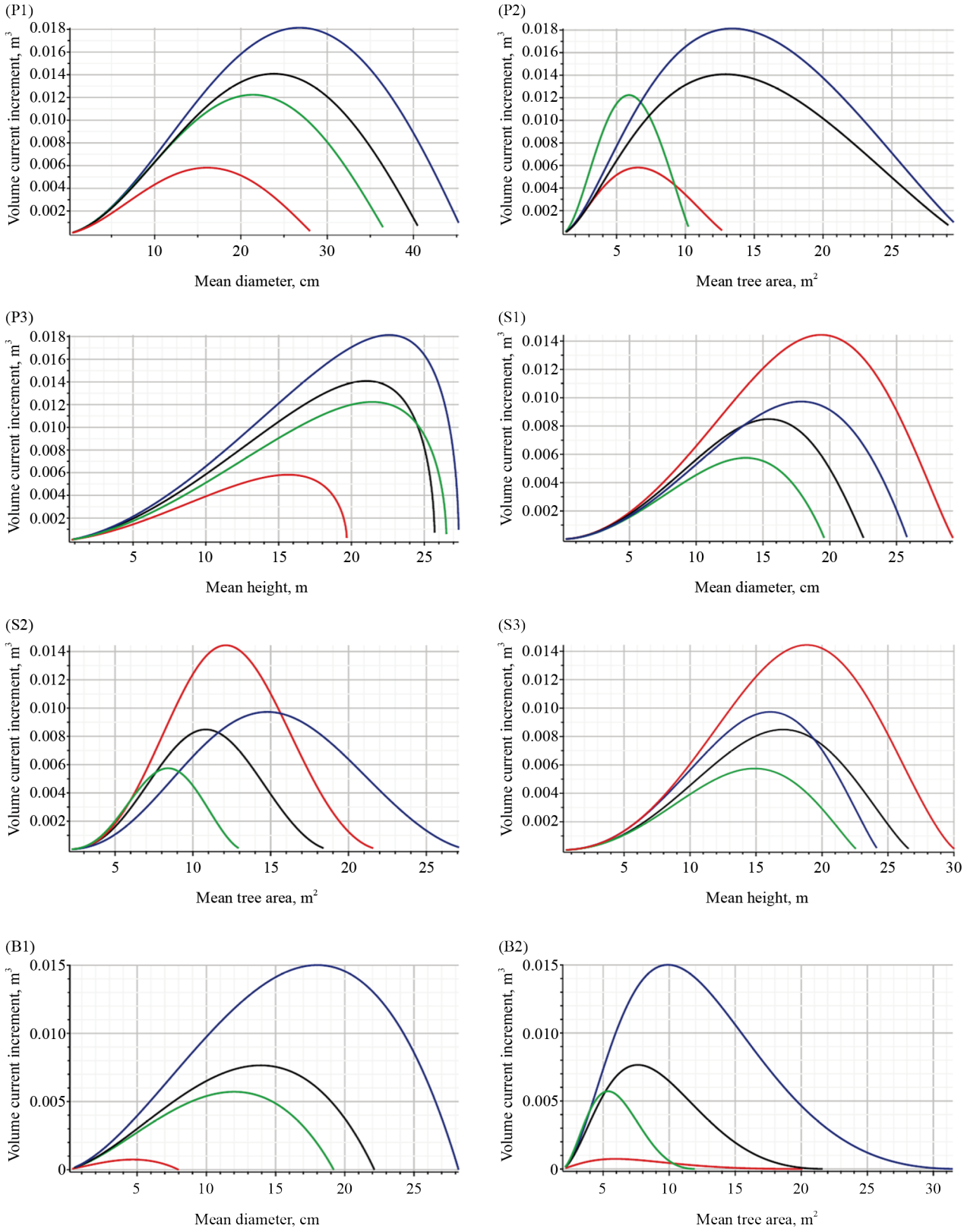
(P1)
Volume current increment, m3
Mean diameter, cm
(P2)
Volume current increment, m3
Mean tree area, m2
(P3)
Volume current increment, m3
Mean height, m
(S1)
Volume current increment, m3
Mean diameter, cm
(S2)
Volume current increment, m3
Mean tree area, m2
(S3)
Volume current increment, m3
Mean height, m
(B1)
Volume current increment, m3
Mean diameter, cm
(B2)
Volume current increment, m3
Mean tree area, m2

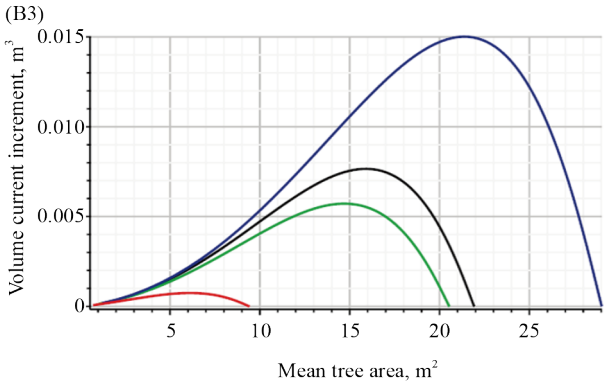

Figure 7. Curves of the mean tree volume's current annual increment over tree size variables (diameter, occupied area, and height) for live trees of pine, spruce, and birch species: (P1, S1, B1) the mean tree volume's current annual increment over tree diameter for three different plots; (P2, S2, B2) the mean tree volume's current increment over tree occupied area for three different plots; (P3, S3, B3) the mean tree volume's current increment over tree height for three different plots; (P1, P2, P3) pine species: in red—the first stand (pine 100%); in blue—the second stand (pine 60%, spruce 3%, birch 37%); in green—the third stand (pine 25%, spruce 72%, birch 3%); (S1, S2, S3) spruce species: in red—the first stand (pine 25%, spruce 75%); in blue—the second stand (pine 40%, spruce 50%, birch 10%); in green—the third stand (pine 60%, spruce 3%, birch 37%); (B1, B2, B3) birch species: in red—the first stand (pine 48%; spruce 13%; birch 39%); in blue—the second stand (pine 73%, birch 27%); in green—the third stand (pine 30%, spruce 61%, birch 9%)

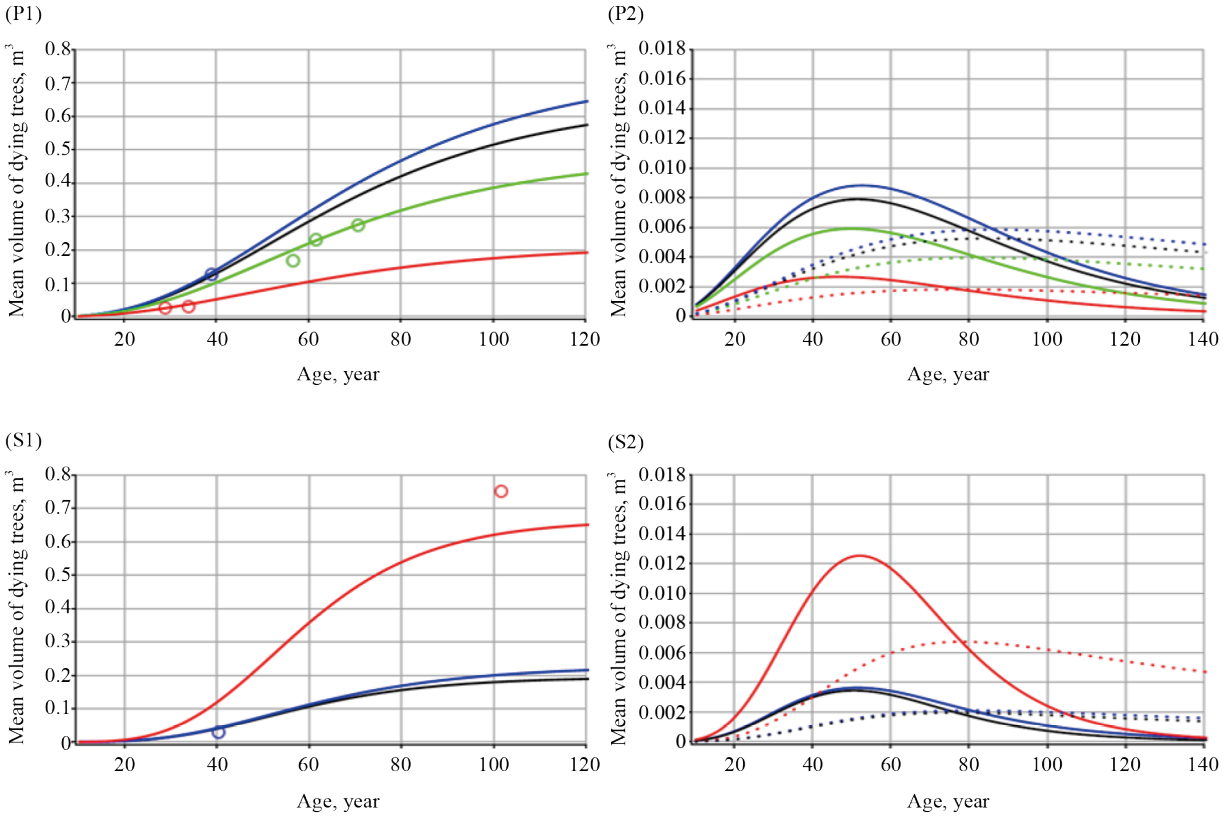

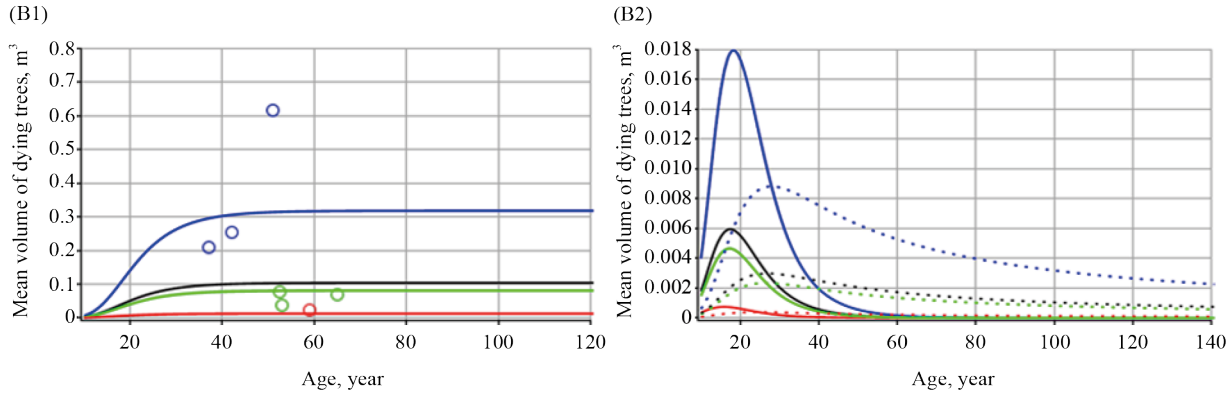

Figure 8. Trajectories of the mean volume and their current and mean increments for pine, spruce, and birch species dying trees: (P1, S1, B1) the mean tree volume: in black—fixed effects mode, and in red, blue, and green—mixed effects mode for three different plots; in circles—the observed values; (P2, S2, B2) the mean tree volume's current, and mean increments: in black—fixed effects mode, and in red, blue and green—mixed effects mode for three different plots; solid line—current annual increment; dotted line—mean annual increment; (P1, P2) pine species: in red—the first stand (pine 100%); in blue—the second stand (pine 60%, spruce 3%, birch 37%); in green—the third stand (pine 25%, spruce 72%, birch 3%); (S1, S2) spruce species: in red—the first stand (pine 25%, sprue 75%); in blue—the second stand (pine 40%, spruce 50%, birch 10%); in green—the third stand (pine 60%, spruce 3%, birch 37%)—no dead trees were recorded; (B1, B2) birch species: in red—the first stand (pine 100%); in blue—the second stand (pine 60%, spruce 3%, birch 37%); in green—the third stand (pine 25%, spruce 72%, birch 3%)

The behavior of a group of trees and the mortality of individual trees both have an impact on the growth response of the surrounding trees, which is a highly complex process. In Figure 8, we concentrate on the growth features of dying trees and compare them with the development of living trees instead of investigating the factors affecting the processes of natural thinning of trees in stands. Dynamical curves of the mean tree volume of dying trees (8P1, 8S1, and 8B1) and corresponding curves of living trees (5P1, 5S1, and 5B1) show that the mean volume of live trees is more than two times the volume of dying trees. The current annual increment and mean annual increment curves for dead trees are displayed in Figures 8P2, 8S2, and 8B2. At their peak, these curves are twice as low as those for equivalent living trees in Figures 5P2, 5S2, and 5B2. Dying trees reach the peak of the current annual increment in a shorter time, as shown in Figures 8P2, 8S2, 8B2, 5P2, 5S2, and 5B2; specifically, pine trees accelerate the peak by approximately 15 years, spruce trees accelerate by 20 years, and birch trees accelerate by 30 years. Birch trees undergo an overwhelming feeling of deterioration before other tree species do, as seen in Figures 8P2, 8S2, and 8B2. A comparison of Figures 8P2, 8S2, and 8B2 reveals that the peak of the current annual increment in the mean volume of spruce trees is the lowest compared with that of other tree species in this region (fixed effects mode).

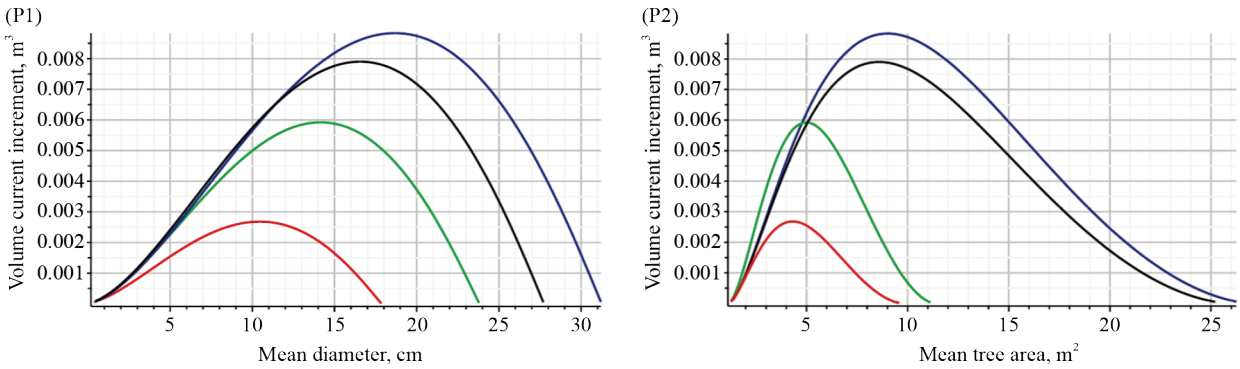

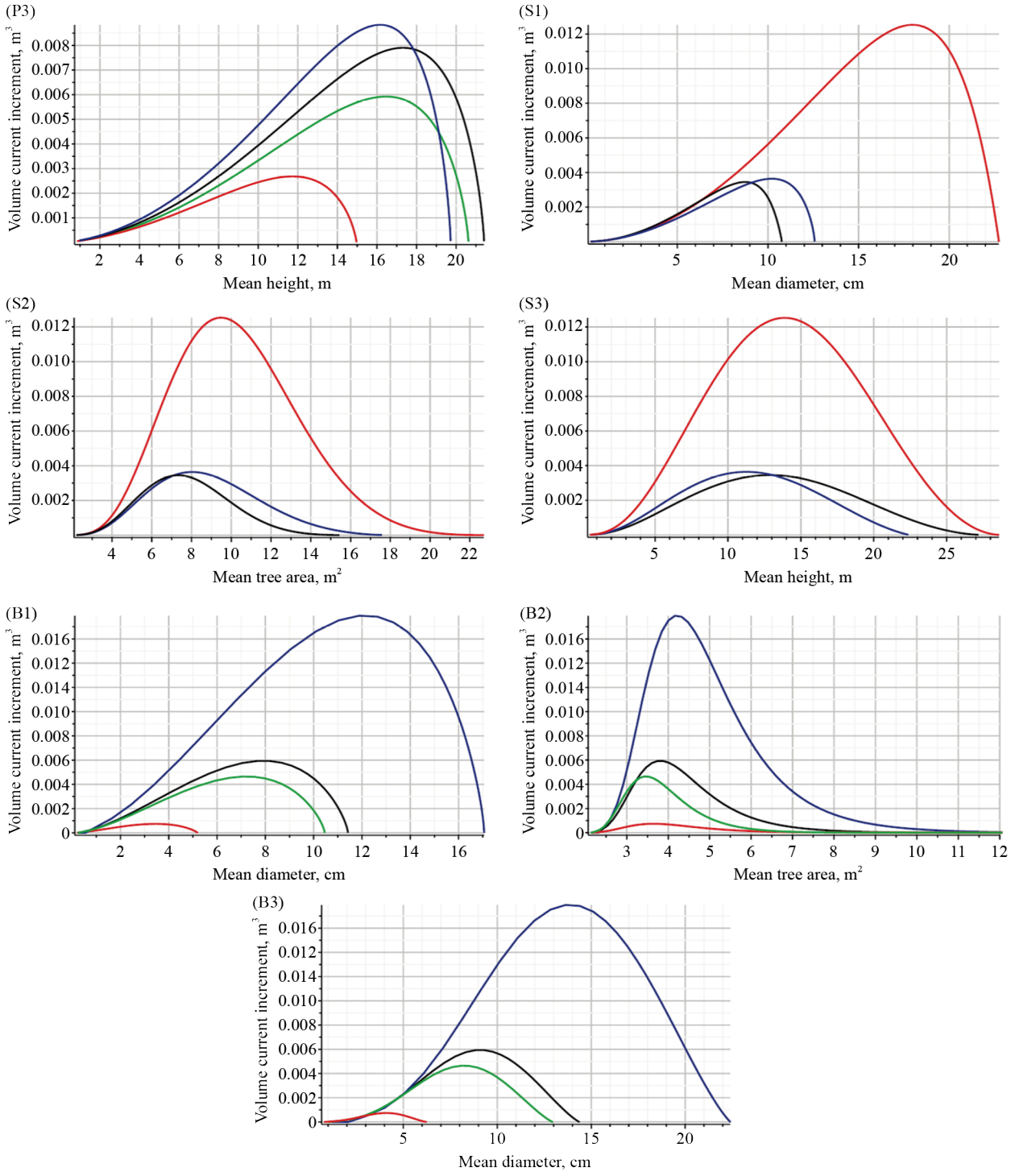

Figure 9. Curves of the mean tree volume's current annual increment over mean tree size variables (diameter, occupied area, and height) for pine, spruce, and birch species dying trees: (P1, S1, B1) the mean tree volume's current annual increment over mean tree diameter for three different plots; (P2, S2, B2) the mean tree volume's current annual increment over mean tree occupied area for three different plots; (P3, S3, B3) the mean tree volume's current annual increment over mean tree height for three different plots; (P1, P2, P3) pine species: in red—the first stand (pine 100%); in blue—the second stand (pine 60%, spruce 3%, birch 37%); in green—the third stand (pine 25%, spruce 72%, birch 3%); (S1, S2, S3) spruce species: in red—the first stand (pine 25%, sprue 75%); in blue—the second stand (pine 40%, spruce 50%, birch 10%); in green—the third stand (pine 60%, spruce 3%, birch 37%); (B1, B2, B3) birch species: in red—the first stand (pine 48%; spruce 13%; birch 39%); in blue—the second stand (pine 73%, birch 27%); in green—the third stand (pine 30%, spruce 61%, birch 9%)

In natural forests, the tree volume of the dying trees is not constant from the beginning of establishment because their volume increases steadily until a certain age when the current annual increment in volume reaches its peak. After this, the tree tends to degrade strongly. Figure 9 highlights the link between the mean tree size variables and the current annual increment in the mean volume of the dying trees. Figure 9 shows how the growth curves asymptotes of the mean tree diameter, occupied area, and height for the dying trees differed considerably for different stands and tree species, as seen from the relationships in Figure 9, where the curves approach the x-axis. Figure 9 shows that the current annual increment in the mean tree volume of trees reaches a maximum in different plots with different mean tree diameters, occupied areas, and heights. Additionally, the mean tree volume current annual increment is peaked by pine trees when the mean tree diameter is between 10 and 20 cm, the mean occupied area is between 4 and 10 m^2, and the mean height is between 12 and 18 m; by spruce trees, when the mean tree diameter is between 8 and 20 cm, the mean occupied area is between 7 and 12 m^2, and the mean height is between 10 and 20 m; and by birch trees, when the mean tree diameter is between 4 and 13 cm, the mean occupied area is between 4 and 15 m^2, and the mean height is between 3 and 14 m. As illustrated in Figure 9, the asymptote of the mean tree diameter, occupied area, and height in a plot increases with the maximum current annual increment in volume that the trees in the plot reach.

Table 5 displays a statistical evaluation of the mean volume of trees prediction accuracy using statistical metrics based on the recently developed mixed-effects parameter diffusion model. The fixed effect parameter estimates from Tables 3 and 4 are utilized, and the observed datasets are used to calibrate the random effects for height and diameter. The provided model demonstrated high goodness-of-fit statistical measures for the predicted mean volume of trees in this area. For example, the root mean square error (percentage root mean square errors) for all, pine, spruce, and birch species were 0.107 m^3 (23.7%), 0.042 m^3 (6.9%), 0.65 m^3 (28.7%), and 0.069 m^3 (19.8%), respectively; and the coefficient of determination for all, pine, spruce, and birch species were 88.3%, 99.1%, 93.2%, and 95.2%, respectively.

Table 5. Statistical measures* for the mean volume model (mixed-effects scenario) of the living trees defined by Equation (10)

Tree species	B (%)	AB (%)	RMSE (%)	R^2
All	−0.0470 (−10.4)	0.0833 (18.4)	0.1073 (23.7)	0.8834
Pine	−0.0096 (−1.5)	0.0268 (4.3)	0.0428 (6.9)	0.9910
Spruce	−0.0283 (−12.4)	0.0449 (19.7)	0.0653 (28.7)	0.9319
Birch	0.0053 (1.5)	0.0439 (12.4)	0.0696 (19.7)	0.9524

*Statistical measures: the mean Bias, B (the percentage mean Bias, % B); the Absolute mean Bias, AB (the percentage Absolute mean Bias, % AB); the Root Mean Square Error, RMSE (the percentage Root Mean Square Error, % RMSE) and the coefficient of determination, R^2

$$\mathrm{B} = \frac{1}{n}\sum_{i=1}^{n}(y_i - \hat{y}_i), \quad \left(\%\,\mathrm{B} = \frac{1}{n}\sum_{i=1}^{n}\frac{y_i - \hat{y}_i}{y_i} \times 100\right), \tag{21}$$

$$\mathrm{AB} = \frac{1}{n}\sum_{i=1}^{n}|y_i - \hat{y}_i|, \quad \left(\%\,\mathrm{B} = \frac{1}{n}\sum_{i=1}^{n}\left|\frac{y_i - \hat{y}_i}{y_i}\right| \times 100\right), \tag{22}$$

$$\mathrm{RMSE} = \sqrt{\frac{1}{n}\sum_{i=1}^{n}(y_i - \hat{y}_i)^2}, \quad \left(\%\,\mathrm{RMSE} = \sqrt{\frac{1}{n}\sum_{i=1}^{n}\left(\frac{y_i - \hat{y}_i}{y_i}\right)^2} \times 100\right), \tag{23}$$

$$R^2 = 1 - \frac{\sum_{i=1}^{n} \left(y_i - \hat{y}_i\right)^2}{\sum_{i=1}^{n} \left(y_i - \bar{y}\right)^2}. \tag{24}$$

The mean tree volume in earlier models was determined by dividing the total volume of all trees by the number of trees in the forest stand. This resulted in the average volume of a tree in the stand. In previous papers, a static and deterministic modeling environment was relied upon to estimate the average tree volume. It is challenging to assess dynamics without making many exact assumptions about how the trees move with age and interact under substantially changing conditions, since we can never know even approximately the majority of the factors involved. Species mixing and tree size diversity are the main drivers of variability in tree production, as they are linked to increases in light-use efficiency or absorbed photosynthetically active radiation. It is appropriate to incorporate the impacts of stochastic noise on the tree size variables, such as diameter, occupied area, and height, since a deterministic system would not be able to account for these environmental forces. The dynamics of the mean volume of live and dying trees determine the mean volume of a forest stand, the monetary value of the standing and dying timber in a forest, the development of forest management plans, the assessment of the growing and dying stock, the absorption and release of CO_2, and the monitoring of changes in the forest over time.

Trees can potentially trap atmospheric carbon through the photosynthesis process, which involves the conversion of carbon from carbon dioxide (CO_2) to carbohydrates that are stored in the leaves, stems, branches, and roots, and contribute to a plant's growth [40]. The total carbon stock in forest stands comprises living trees, standing dead trees, and fallen dead wood. The developed mean tree volume trajectories for both living and dying trees in this study may be used to calculate the total mean tree biomass using a biomass expansion factor, and then estimate the carbon content by multiplying the biomass by the carbon fraction factor.

5. Conclusions

The composition and structure of a stand's live and dying trees are dynamic, always evolving or changing in response to environmental disturbances. In this study, the growth processes of all tree size variables (diameter, occupied area, and height) were adapted using the sigmoidal, 4-parameter Gompertz-type univariate stochastic differential equation. These equations are linked to a trivariate stochastic process via all bivariate correlations. Since the newly created mean tree volume model is based on the growth and death of individual trees, it may be referred to as the "individual tree model". The features of individual tree models allow the formulation of aggregate models that describe the stands' yield and growth. The newly presented model confirms that the mean volume trajectory of trees in a forest stand may be tracked and described with increasing tree age. These results have important implications for forecasting a forest stand's mean tree volume and improving forest management techniques. This work contributes significantly by successfully transforming the analysis of tree size variables (height and diameter) into stochastic processes that make possible the description of mean tree volume changes via age. Most previous mean tree volume and other tree attribute models that forest statisticians provide are static, even-aged, and 'data-driven' (based on measurements taken on the ground or remotely) [41, 42].

The mixed-effect parameters Gompertz-type process model has proven to be highly adaptable and attractive. There are still a lot of modeling and computational issues to be resolved, yet. Further studies should focus on expanding that model by considering the mean volume per hectare of a forest stand for mixed species and uneven-aged stands. By adding other tree size variables to the mean tree volume model, such as the crown area and crown base height, it would be possible to use conditional distributions to better understand how these variables affect mean tree volume. It would be natural for future research to examine the potential use involving various diffusion processes, such as von Bertalanffy [43], Vasicek inhomogeneous [44], and others. As forests face increasing dangers from climate change and other environmental problems, it becomes crucial to apply effective modeling tools, formulated by using multi-dimensional diffusion processes, to fully understand the perspectives of forest resources.

Acknowledgments

The author would like to thank the anonymous reviewers for their time and effort in reviewing the work. I deeply value all constructive feedback and recommendations. I thank the Edmundas Petrauskas research group for their help with field sampling (Project: M-04-09/19, Vytautas Magnus University).

Funding

This research paper received funding from the Horizon Europe Framework Programme (HORIZON), called Teaming for Excellence (HORIZON-WIDERA-2022-ACCESS-01-two-stage)—Creation of the Centre of Excellence in Smart Forestry "Forest 4.0" No. 101059985. This research was complementary funded by the European Union under the project "FOREST 4.0—Center of Excellence for the Development of a Sustainable Forest Bioeconomy", No. 10-042-P-0002.

Conflict of interest

The authors declare no competing financial interest.

References

[1] Garcia O. On bridging the gap between tree-level and stand-level models. In: *Proceedings of IUFRO 4.11 Conference: Forest Biometry, Modeling and Information Science*. UK: University of Greenwich; 2001. p.311-323.

[2] Maleki K, Astrup R, Kuehne C, McLean JP, Antón-Fernández C. Stand-level growth models for long-term projections of the main species groups in Norway. *Scandinavian Journal of Forest Research*. 2022; 37(2): 130-143. Available from: https://doi.org/10.1080/02827581.2022.2056632.

[3] Viet HDX, Tymińska-Czabańska L, Socha J. Modeling the effect of stand characteristics on oak volume increment in Poland using generalized additive models. *Forests*. 2023; 14(1): 123. Available from: https://doi.org/10.3390/f14010123.

[4] Egusa T, Nakahata R, Neumann M, Kumagai T. Carbon stock projection for four major forest plantation species in Japan. *Science of The Total Environment*. 2024; 927: 172241. Available from: https://doi.org/10.1016/j.scitotenv.2024.172241.

[5] Lewis SL, Wheeler CE, Mitchard ETA, Koch A. Restoring natural forests is the best way to remove atmospheric carbon. *Nature*. 2019; 568: 25-28. Available from: https://doi.org/10.1038/d41586-019-01026-8.

[6] Singh H, Tiwari SC. Carbon stock and carbon sequestration potential of forest growing stock around National Thermal Power Plant, Bilaspur, Chhattisgarh, Central India. *Forestist*. 2024; 74: 289-297. Available from: https://doi.org/10.5152/forestist.2024.23052.

[7] Strîmbu VF, Eid T, Gobakken T. A stand level scenario model for the Norwegian forestry—a case study on forest management under climate change. *Silva Fennica*. 2023; 57(2): 23019. Available from: https://doi.org/10.14214/sf.23019.

[8] Chicco D, Warrens MJ, Jurman G. The coefficient of determination R-squared is more informative than SMAPE, MAE, MAPE, MSE and RMSE in regression analysis evaluation. *PeerJ Computer Science*. 2021; 7: e623. Available from: https://doi.org/10.7717/peerj-cs.623.

[9] Sen A, Srivastava M. *Regression Analysis—Theory, Methods, and Applications*. Berlin, Germany: Springer-Verlag; 2011.

[10] Odunayo BJ, Nnamdi E, Correa FM. Initial growth rate and model performance for COVID-19 in Nigeria. *Contemporary Mathematics*. 2025; 6(2): 2377-2391. Available from: https://doi.org/10.37256/cm.6220255889.

[11] Battaglia M, Sands P. Process-based forest productivity models and their application in forest management. *Forest Ecology and Management*. 1998; 102(1): 13-32. Available from: https://doi.org/10.1016/S0378-1127(97)00112-6.

[12] Garcia O. Modeling with stochastic differential equations. *Mathematical and Computational Forestry and Natural-Resource Sciences*. 2024; 16(2): 27-32.
[13] Rennolls K. Forest height growth modelling. *Forest Ecology and Management*. 1995; 71(3): 217-225. Available from: https://doi.org/10.1016/0378-1127(94)06102-O.
[14] Rupšys P. Compatible basal area models for live and dying trees using diffusion processes. *Journal of Forestry Research*. 2025; 36: 36. Available from: https://doi.org/10.1007/s11676-025-01829-8.
[15] Suzuki T. Forest transition as a stochastic process I. *Journal of Japanese Forestry Society*. 1966; 48: 436-439.
[16] Aït-Sahalia Y, Kimmel R. Maximum likelihood estimation of stochastic volatility models. *Journal of Financial Economics*. 2007; 83(2): 413-452. Available from: https://doi.org/10.1016/j.jfineco.2005.10.006.
[17] Cao Y, Fu J. Stationary distribution and density function analysis of stochastic SIQS epidemic model with Markov chain. *International Journal of Biomathematics*. 2024; 17: 2350062. Available from: https://doi.org/10.1142/S1793524523500626.
[18] Saravanan S, Monica C. Dynamic analysis of extinction and stationary distribution of a stochastic dual-strain SEIR epidemic model with double saturated incidence rates. *Contemporary Mathematics*. 2024; 5(4): 6130-6164. Available from: https://doi.org/10.37256/cm.5420245594.
[19] Petrauskas E, Rupšys P. Diffusion mechanisms for both living and dying trees across 37 years in a forest stand in Lithuania's Kazlų Rūda region. *Symmetry*. 2025; 17(2): 213. Available from: https://doi.org/10.3390/sym17020213.
[20] Rupšys P. Modeling dynamics of structural components of forest stands based on trivariate stochastic differential equation. *Forests*. 2019; 10(6): 506. Available from: https://doi.org/10.3390/f10060506.
[21] Rupšys P, Mozgeris G, Petrauskas E, Krikštolaitis R. A framework for analyzing individual-tree and whole-stand growth by fusing multilevel data: stochastic differential equation and copula network. *Forests*. 2023; 14(10): 2037. Available from: https://doi.org/10.3390/f14102037.
[22] Alegria C, Tomé M. A set of models for individual tree merchantable volume prediction for *Pinus pinaster* Aiton in central inland of Portugal. *European Journal of Forest Research*. 2011; 130: 871-879. Available from: https://doi.org/10.1007/s10342-011-0479-3.
[23] Cao QV. Linking individual-tree and whole-stand models for forest growth and yield prediction. *Forest Ecosystems*. 2014; 1: 18. Available from: https://doi.org/10.1186/s40663-014-0018-z.
[24] Rupšys P, Petrauskas E. Development of *q*-exponential models for tree height, volume, and stem profile. *International Journal of the Physical Sciences*. 2010; 5(15): 2369-2378.
[25] Monagan MB, Geddes KO, Heal KM, Labahn G, Vorkoetter SM, Mccarron J. *Maple Advanced Programming Guide*. Waterloo, Canada: Maplesoft; 2007.
[26] Li Y, Li J, Wei L. Stable reverse *J*-shaped diameter distribution occurs in an old-growth karst forest. *Journal of Forestry Research*. 2024; 35: 107. Available from: https://doi.org/10.1007/s11676-024-01763-1.
[27] Mønness E. The bivariate power-normal distribution and the bivariate Johnson system bounded distribution in forestry, including height curves. *Canadian Journal of Forest Research*. 2015; 45(3): 307-313. Available from: https://doi.org/10.1139/cjfr-2014-0333.
[28] Kelemen S, Józsa M, Hartel T, Csóka G, Néda Z. Tree size distribution as the stationary limit of an evolutionary master equation. *Scientific Reports*. 2024; 14: 1168. Available from: https://doi.org/10.1038/s41598-024-51553-2.
[29] Krikštolaitis R, Mozgeris G, Petrauskas E, Rupšys P. A statistical dependence framework based on a multivariate normal copula function and stochastic differential equations for multivariate data in forestry. *Axioms*. 2023; 12(5): 457. Available from: https://doi.org/10.3390/axioms12050457.
[30] Pommerening A, Szmyt J, Duchiron MS. Revisiting silvicultural systems: towards a systematic and generic design of tree regeneration methods. *Trees Forests and People*. 2024; 17: 100597. Available from: https://doi.org/10.1016/j.tfp.2024.100597.
[31] Itó K. On stochastic differential equations. *Memoirs of the American Mathematical Society*. 1951; 4: 1-51.
[32] Narmontas M, Rupšys P, Petrauskas E. Models for tree taper form: the Gompertz and Vasicek diffusion processes framework. *Symmetry*. 2020; 12(1): 80. Available from: https://doi.org/10.3390/sym12010080.
[33] Rupšys P, Petrauskas E. On the construction of growth models via symmetric copulas and stochastic differential equations. *Symmetry*. 2022; 14(10): 2127. Available from: https://doi.org/10.3390/sym14102127.
[34] Fisher RA. On the mathematical foundations of theoretical statistics. *Philosophical Transactions of the Royal Society of London, Series A*. 1922; 222: 309-368. Available from: https://doi.org/10.1098/rsta.1922.0009.

[35] Bonett DG. Meta-analytic interval estimation for bivariate correlations. *Psychological Methods*. 2008; 13(3): 173-181. Available from: https://doi.org/10.1037/a0012868.

[36] Österberg N, Parkatti VP, Tahvonen O. Comparing stand growth models in optimizing mixed-species forest management. *Scandinavian Journal of Forest Research*. 2023; 38(6): 353-366. Available from: https://doi.org/10.1080/02827581.2023.2227095.

[37] Harayama H, Yamada T, Kitao M, Tsuyama I. Analysis of height and diameter growth patterns in Sakhalin fir seedlings competing with evergreen dwarf bamboo and deciduous vegetation using generalized additive models. *Journal of Forestry Research*. 2025; 36: 63. Available from: https://doi.org/10.1007/s11676-025-01858-3.

[38] Hunt R. Plant growth analysis: second derivatives and compounded second derivatives of splined plant growth curves. *Annals of Botany*. 1982; 50(3): 317-328. Available from: https://doi.org/10.1093/oxfordjournals.aob.a086371.

[39] Rupšys P. New insights into tree height distribution based on mixed effects univariate diffusion processes. *PLoS ONE*. 2016; 11(12): e0168507. Available from: https://doi.org/10.1371/journal.pone.0168507.

[40] McClory R, Ellis RH, Lukac M, Clark J, Mayoral C, Hart KM, et al. Carbon dioxide enrichment affected flower numbers transiently and increased successful post-pollination development stably but without altering final acorn production in mature pedunculate oak (*Quercus robur* L.). *Journal of Forestry Research*. 2024; 35: 73. Available from: https://doi.org/10.1007/s11676-024-01724-8.

[41] Kangas A, Pitkänen TP, Mehtätalo L, Heikkinen J. Mixed linear and non-linear tree volume models with regional parameters to main tree species in Finland. *Forestry: An International Journal of Forest Research*. 2023; 96(2): 188-206. Available from: https://doi.org/10.1093/forestry/cpac038.

[42] Umemi K, Inoue A. A model for predicting mean diameter at breast height from mean tree height and stand density. *Journal of Forest Research*. 2024; 29(3): 186-195. Available from: https://doi.org/10.1080/13416979.2024.2311946.

[43] Rupšys P, Petrauskas E. Evolution of the bivariate tree diameter and height distributions via the stand age: von Bertalanffy bivariate diffusion process approach. *Journal of Forest Research*. 2018; 24(1): 16-26. Available from: https://doi.org/10.1080/13416979.2018.1544433.

[44] Makhlouki N, Nafidi A, Makroz I, Sánchez RG. A new inhomogeneous Vasicek model: statistical treatment, simulation study and application. *Advances and Applications in Statistics*. 2025; 92(7): 1075-1092. Available from: https://doi.org/10.17654/0972361725048.